

Four-loop lattice-regularized vacuum energy density of the three-dimensional $SU(3)$ + adjoint Higgs theory

F. Di Renzo^a, M. Laine^{b,c}, Y. Schröder^b, C. Torrero^d

^a*Università di Parma & INFN, I-43100 Parma, Italy*

^b*Faculty of Physics, University of Bielefeld, D-33501 Bielefeld, Germany*

^c*Department of Physics, University of Oulu, FI-90014 Oulu, Finland*

^d*Institute for Theoretical Physics, University of Regensburg, D-93040 Regensburg, Germany*

Abstract

The pressure of QCD admits at high temperatures a factorization into purely perturbative contributions from “hard” thermal momenta, and slowly convergent as well as non-perturbative contributions from “soft” thermal momenta. The latter can be related to various effective gluon condensates in a dimensionally reduced effective field theory, and measured there through lattice simulations. Practical measurements of one of the relevant condensates have suffered, however, from difficulties in extrapolating convincingly to the continuum limit. In order to gain insight on this problem, we employ Numerical Stochastic Perturbation Theory to estimate the problematic condensate up to 4-loop order in lattice perturbation theory. Our results seem to confirm the presence of “large” discretization effects, going like $a \ln(1/a)$, where a is the lattice spacing. For definite conclusions, however, it would be helpful to repeat the corresponding part of our study with standard lattice perturbation theory techniques.

1. Introduction

Given possible applications in cosmology and in the phenomenology of heavy ion collision experiments, as well as the important theoretical role that the free energy density plays in understanding the properties of any finite-temperature system, the pressure (or minus the free energy density) of Quantum Chromodynamics (QCD) is one of the central observables of relativistic thermal field theory. In this paper we focus on its determination at temperatures above a few hundred MeV, where the system is deconfined; there, if anywhere, it should eventually be possible to establish a quantitative first-principles description in terms of the temperature and the fundamental parameters of the theory.

Given the importance of the problem, a huge amount of work has already been carried out on the topic. (The references most directly related to the present work are cited at the beginning of the next section.) In general, the approaches can be divided into numerical (i.e. lattice Monte Carlo) and analytic (i.e. weak-coupling expansion or various improvements thereof) techniques. In addition, there is a strategy — the one that we follow here — which combines elements from both sides. The idea is to factorise the system into two parts: “hard” momenta, whose contribution is perturbative, and “soft” momenta, which need to be treated non-perturbatively. (One benefit of this approach is that dynamical quarks remain cheap even in the chiral continuum limit, since only gauge fields possess soft momenta.) Our study concerns the non-perturbative soft part, but not directly its lattice measurement; rather, the point is that for such a factorization to work, both sides of the result need to be converted to the same regularization scheme, so that they can be added together. In some situations, like in ours, such a scheme conversion can turn out to be technically as demanding as the non-perturbative measurement itself, and this is the ultimate challenge that we try to tackle in this work.

This paper is organised as follows. The general setup of factorising the pressure to contributions from perturbatively computable terms, and ones that need to be estimated numerically, as well as the role that the present study plays in this setup, is outlined in Sec. 2. The outline is made quantitative in Sec. 3, where we define the precise quantities that we want to determine. The tool used for the computation, Numerical Stochastic Perturbation Theory, is reviewed in Sec. 4. The numerical data is analysed in Sec. 5; our results and conclusions comprise Sec. 6. In three appendices, we detail the perturbative expressions that we have worked out explicitly in lattice regularization.

2. Outline of setup

At a high temperature T and a small gauge coupling constant g , there are parametrically three different momentum scales in hot QCD: $k \sim \pi T, gT, g^2 T/\pi$ [1]. All the effects of the hard scale, $k \sim \pi T$, can be accounted for by a method called dimensional reduction [1, 2]. In

particular, the pressure, or minus the free energy density, can be written as [3]

$$p_{\text{QCD}}(T) \equiv p_{\text{E}}(T) + \lim_{V \rightarrow \infty} \frac{T}{V} \ln \int \mathcal{D}A_i^a \mathcal{D}A_0^a \exp(-S_{\text{E}}), \quad (2.1)$$

where V is the volume, A_i^a are gauge fields, A_0^a are scalar fields in the adjoint representation, and S_{E} is a three-dimensional effective field theory, to be specified presently (the subscript may refer to ‘‘Electrostatic QCD’’ [3]). The function $p_{\text{E}}(T)$ gets contributions only from the hard scale, $k \sim \pi T$, and is computable in perturbation theory; the path integral with S_{E} contains the contributions of the soft modes, $k \sim gT, g^2T/\pi$, and should preferably be determined non-perturbatively (the contributions from the modes $k \sim g^2T/\pi$ are genuinely non-perturbative [4, 5]; those from the modes $k \sim gT$ are in principle still perturbative, but in general slowly convergent [3], [6]–[9], although some observables with possibly faster convergence have also been found [10]). The same description applies also in the presence of a small quark chemical potential [11], allowing to compute further quantities such as quark number susceptibilities [12]. At least when treated non-perturbatively, Electrostatic QCD appears to yield a quantitative description of the full four-dimensional theory up from about $T \sim 1.5T_c$, where T_c denotes the pseudocritical temperature of the QCD crossover (see, e.g., ref. [13] and references therein).

Now, to give a precise meaning to Eq. (2.1), requires the specification of a regularization scheme. Though a purely perturbative challenge, the determination of $p_{\text{E}}(T)$ is fairly complicated in practice [6]. Therefore, it is preferable to use dimensional regularization for the algebra: all the 3-loop and 4-loop results available today have been obtained in the $\overline{\text{MS}}$ scheme [3], [6]–[8], [14, 15].

Let us, correspondingly, denote the $\overline{\text{MS}}$ scheme ‘‘vacuum energy density’’ of the theory defined by S_{E} , with

$$f_{\overline{\text{MS}}} \equiv - \left\{ \lim_{V \rightarrow \infty} \frac{1}{V} \ln \int \mathcal{D}A_i^a \mathcal{D}A_0^a \exp(-S_{\text{E}}) \right\}_{\overline{\text{MS}}}, \quad (2.2)$$

where $V = \int d^d \mathbf{x}$ is the d -dimensional volume. Then Eq. (2.1) becomes

$$p_{\text{QCD}}(T) = \left\{ p_{\text{E}}(T) \right\}_{\overline{\text{MS}}} - T f_{\overline{\text{MS}}}. \quad (2.3)$$

Though each part is scheme-dependent, the expression as a whole is not. In the following, we concentrate exclusively on the determination of $f_{\overline{\text{MS}}}$.

To take further steps, we need to specify the effective action S_{E} . It reads

$$S_{\text{E}} = \int d^d x \mathcal{L}_{\text{E}}, \quad (2.4)$$

$$\mathcal{L}_{\text{E}} = \frac{1}{2} \text{Tr} [F_{ij}^2] + \text{Tr} [D_i, A_0]^2 + m_3^2 \text{Tr} [A_0^2] + \lambda_3 (\text{Tr} [A_0^2])^2 + \dots \quad (2.5)$$

Here $i = 1, \dots, d$, $d = 3 - 2\epsilon$, $F_{ij} = (i/g_3)[D_i, D_j]$, $D_i = \partial_i - ig_3 A_i$, $A_i = A_i^a T^a$, $A_0 = A_0^a T^a$, and T^a are hermitean generators of $SU(N_c)$, normalised as $\text{Tr}[T^a T^b] = \delta^{ab}/2$.¹ The dimensionalities of g_3^2 and λ_3 are $\text{GeV}^{1+2\epsilon}$. There are also higher order operators, classified in ref. [17], whose parametric importance has been analysed in ref. [8]; even though some of them contribute at the same parametric order as some of the effects that we are after, it is still a well-defined problem to start by determining the full non-perturbative effect of the truncated form of the theory in Eq. (2.5). Therefore we will ignore all higher order operators in the following.

Now, $f_{\overline{\text{MS}}}$ may include a part which is independent of m_3^2 . However, this part can be evaluated by sending $m_3^2 \rightarrow \infty$, whereby the field A_0 can be integrated out. Thereby the problem reduces to that already considered in refs. [18, 14]. In the following, we concentrate on the part of $f_{\overline{\text{MS}}}$ which does depend on m_3^2 .

The part of $f_{\overline{\text{MS}}}$ depending on m_3^2 can be isolated through a partial derivative, which in turn yields a condensate:²

$$\partial_{m_3^2} f_{\overline{\text{MS}}} = \left\langle \text{Tr}[A_0^2] \right\rangle_{\overline{\text{MS}}}. \quad (2.6)$$

Thus, if we are able to measure the condensate $\langle \text{Tr}[A_0^2] \rangle$ in lattice regularization, and convert the result to the $\overline{\text{MS}}$ scheme, we are able to determine the m_3^2 -dependent part of $f_{\overline{\text{MS}}}$ non-perturbatively. In principle this is, indeed, doable: the relation of the two regularization schemes, which is exact in the continuum limit due to the super-renormalizability of the theory in Eq. (2.5), can be found in refs. [21, 22] (see also Eq. (3.12) below).

Let us be a bit more specific about what we would like to achieve with the lattice simulations. Note first that in the $\overline{\text{MS}}$ scheme, the m_3^2 -dependent part of $f_{\overline{\text{MS}}}$ is known analytically up to 4-loop order [23]. This corresponds to an expansion of the form

$$\left\langle \text{Tr}[A_0^2] \right\rangle_{\overline{\text{MS}}} = m_3 + g_3^2 \ln \frac{\bar{\mu}}{m_3} + \frac{g_3^4}{m_3} + \frac{g_3^6}{m_3^2} + \mathcal{O}\left(\frac{g_3^8}{m_3^3}\right), \quad (2.7)$$

where $\bar{\mu}$ is the $\overline{\text{MS}}$ scale parameter, and we have for simplicity omitted all numerical coefficients, as well as terms containing λ_3 . What we would like to determine is the ‘‘remainder’’, i.e. the sum of terms beyond the level that is already known analytically. Denoting by $\langle \text{Tr}[A_0^2] \rangle_a$ the condensate in lattice regularization, and by a the lattice spacing, the remainder is

$$\left\langle \text{Tr}[A_0^2] \right\rangle_{\overline{\text{MS}}}^{\mathcal{R}} \equiv \lim_{a \rightarrow 0} \left\{ \left\langle \text{Tr}[A_0^2] \right\rangle_a - \frac{1}{a} - g_3^2 \ln \frac{1}{a\bar{\mu}} \right\} - m_3 - g_3^2 \ln \frac{\bar{\mu}}{m_3} - \frac{g_3^4}{m_3} - \frac{g_3^6}{m_3^2}, \quad (2.8)$$

where the limit inside the curly brackets takes us to the $\overline{\text{MS}}$ scheme [21, 22], and the subsequent continuum expression subtracts the known terms in Eq. (2.7).

¹In the present paper we concentrate on $N_c = 3$, but lattice measurements have previously been carried out also for $N_c = 2$ [16]. For $N_c \geq 4$, another independent quartic coupling should be included in Eq. (2.5).

²This condensate is analogous to the Polyakov loop condensate, playing a role in various attempts at improved effective theories of hot QCD (see, e.g., refs. [19, 20] and references therein), but it appears difficult to promote the analogy to a precise relation.

The problem with this procedure is that in practice the limit $a \rightarrow 0$ in Eq. (2.8) cannot be taken exactly, but it introduces systematic errors. To carry out the limit requires a fit ansatz; in three dimensions, discretization effects go like $\mathcal{O}(a)$. These dominant errors could in principle be removed through an improvement program [24], but even if it had been completed (which is presently not the case), one would still need an ansatz for the subsequent terms, and at this point it is for instance not clear whether logarithms like $a^2 \ln(1/a)$ should be included. Yet, this may have a noticeable impact on the results. Moreover, the ansatz is necessarily of a finite order; this means that there will remain residual 1-loop discretization errors in the result, while the subsequent subtraction of the continuum terms is attempting to take us to the 5-loop level and beyond. Evidently, this situation is unsatisfactory; for a demonstration of the problems encountered, see ref. [12].

The goal of the present paper is, then, to determine the terms corresponding to those in Eq. (2.7) “exactly” in lattice regularization. That is, we do not carry out any expansion in am_3 ; only one in the loop order. The corresponding result contains the counterterms needed for the limit in Eq. (2.8); the finite terms in Eq. (2.8); but also an infinite number of higher order corrections, starting at $\mathcal{O}(am_3)$. Then, we can write the remainder as

$$\left\langle \text{Tr} [A_0^2] \right\rangle_{\overline{\text{MS}}}^{\mathcal{R}} = \lim_{a \rightarrow 0} \left\{ \left\langle \text{Tr} [A_0^2] \right\rangle_a - m_3 f_0(am_3) - g_3^2 f_1(am_3) - \frac{g_3^4}{m_3} f_2(am_3) - \frac{g_3^6}{m_3^2} f_3(am_3) \right\}, \quad (2.9)$$

where f_i are the functions to be determined. We of course still need to take the limit $a \rightarrow 0$ at the end, as indicated by Eq. (2.9), but we have gained in that we do not need to be as worried about discretization errors as before: any number yielded by the difference inside the curly brackets in Eq. (2.9) is already an approximation for the remainder, and there is no danger of 1-loop discretization errors overtaking an interesting 5-loop continuum effect.

3. Precise setup

Let us now add the missing details to the formulation of the problem. The 4-loop computation of $f_{\overline{\text{MS}}}$ in dimensional regularization has been described in detail in ref. [23]. The mass parameter needs renormalisation,

$$m_{3,\text{bare}}^2 = m_3^2(\bar{\mu}) + \delta m_{\overline{\text{MS}}}^2, \quad (3.1)$$

$$\delta m_{\overline{\text{MS}}}^2 = \frac{1}{(4\pi)^2} \frac{\mu^{-4\epsilon}}{4\epsilon} 2(d_A + 2) \left(-g_3^2 \lambda_3 C_A + \lambda_3^2 \right), \quad (3.2)$$

where $\bar{\mu}^2 \equiv 4\pi\mu^2 e^{-\gamma_E}$, $C_A \equiv N_c$, and $d_A \equiv N_c^2 - 1$. Consequently the renormalised mass parameter satisfies the equation

$$\bar{\mu} \frac{d}{d\bar{\mu}} m_3^2(\bar{\mu}) = \frac{1}{8\pi^2} (d_A + 2) \left(-g_3^2 \lambda_3 C_A + \lambda_3^2 \right). \quad (3.3)$$

Here and in the following, we assume $\epsilon \rightarrow 0$ taken in all finite quantities. It is convenient to define the dimensionless ratios

$$x \equiv \frac{\lambda_3}{g_3^2}, \quad (3.4)$$

$$y \equiv \frac{m_3^2(\bar{\mu} = g_3^2)}{g_3^4}. \quad (3.5)$$

As indicated, we choose $\bar{\mu} \equiv g_3^2$ for defining y .

Now, it is thought that the perturbative series for the pressure of QCD converges very slowly [6, 7]. The reason for this can be traced back to the slow convergence of the perturbative series for $\partial_{m_3^2} f_{\overline{\text{MS}}}$ [3, 25, 8]. Making use of the results of ref. [23], and inserting the choice $\bar{\mu} = g_3^2$, the known 4-loop result can be written as

$$\begin{aligned} \left\langle \text{Tr} [A_0^2/g_3^2] \right\rangle_{\overline{\text{MS}}, \bar{\mu}=g_3^2} &= -\frac{d_A}{(4\pi)} \frac{y^{\frac{1}{2}}}{2} + \\ &+ \frac{d_A}{(4\pi)^2} \frac{1}{4} \left\{ C_A \left[1 - 2 \ln(4y) \right] + x(d_A + 2) \right\} + \\ &+ \frac{d_A}{(4\pi)^3} \frac{1}{4y^{\frac{1}{2}}} \left\{ C_A^2 \left[\frac{89}{12} + \frac{\pi^2}{3} - \frac{11}{3} \ln 2 \right] + x C_A (d_A + 2) \left[\ln(4y) + \frac{3}{2} \right] + \right. \\ &\quad \left. + x^2 (d_A + 2) \left[1 - \ln(16y) \right] - \frac{x^2}{4} (d_A + 2)^2 \right\} + \\ &+ \frac{d_A}{(4\pi)^4} \frac{1}{4y} \left\{ 2C_A^3 \left[\frac{43}{4} - \frac{491}{768} \pi^2 \right] + 10 x C_A^2 \left[1 - \frac{\pi^2}{8} \right] + \right. \\ &\quad \left. + x C_A^2 (d_A + 2) \left[2 \ln(4y) - 1 \right] + \right. \\ &\quad \left. + 2x^2 C_A (d_A + 2) \left[\frac{36 - \pi^2}{8} - \ln(4y) \right] - x^2 C_A (d_A + 2)^2 - \right. \\ &\quad \left. - x^3 (d_A + 2)(d_A + 8) \frac{\pi^2}{12} + x^3 (d_A + 2)^2 \right\}. \quad (3.6) \end{aligned}$$

The terms beyond Eq. (3.6) die away as $y^{-\frac{3}{2}}$ at large y , modulo possible logarithms, but realistic values of y are not that large (for $N_c = 3, N_f = 3, y \simeq 0.39 [\log_{10}(T/\Lambda_{\overline{\text{MS}}}) + 1.0]$). The goal of a non-perturbative determination is therefore to sum the whole series beyond these known terms.

We then move to the lattice side. To this effect, let us define the lattice action, S_a , corresponding to Eq. (2.4). The standard Wilson discretization yields

$$\begin{aligned} S_a &= \beta \sum_{\mathbf{x}} \sum_{i < j} \left\{ 1 - \frac{1}{C_A} \text{Re Tr} [P_{ij}(\mathbf{x})] \right\} + \\ &+ 2a \sum_{\mathbf{x}} \sum_i \left\{ \text{Tr} [A_0^2(\mathbf{x})] - \text{Tr} [A_0(\mathbf{x}) U_i(\mathbf{x}) A_0(\mathbf{x} + i) U_i^\dagger(\mathbf{x})] \right\} + \end{aligned}$$

$$+ a^3 \sum_{\mathbf{x}} \left\{ m_{3,\text{bare}}^2 \text{Tr} [A_0^2(\mathbf{x})] + \lambda_3 \left(\text{Tr} [A_0^2(\mathbf{x})] \right)^2 \right\}, \quad (3.7)$$

where a is the lattice spacing, $U_i(\mathbf{x})$ is a link matrix, $\mathbf{x} + i \equiv \mathbf{x} + a\hat{e}_i$, where \hat{e}_i is a unit vector, $P_{ij}(\mathbf{x})$ is the plaquette, and

$$\beta \equiv \frac{2C_A}{g_3^2 a}. \quad (3.8)$$

The bare mass parameter of Eq. (3.7) reads [22]

$$\begin{aligned} m_{3,\text{bare}}^2 &= m_3^2(\bar{\mu}) + \delta m_a^2, \\ \delta m_a^2 &= - \left[2g_3^2 C_A + \lambda_3(d_A + 2) \right] \frac{\Sigma}{4\pi a} + \\ &+ \frac{1}{(4\pi)^2} \left\{ 2\lambda_3(d_A + 2)(\lambda_3 - g_3^2 C_A) \left(\ln \frac{6}{a\bar{\mu}} + \zeta \right) - 2g_3^2 C_A \lambda_3(d_A + 2) \left(\frac{\Sigma^2}{4} - \delta \right) - \right. \\ &\left. - g_3^4 C_A^2 \left[\frac{5}{8} \Sigma^2 + \left(\frac{1}{2} - \frac{4}{3C_A^2} \right) \pi \Sigma - 4(\delta + \rho) + 2\kappa_1 - \kappa_4 \right] \right\}, \end{aligned} \quad (3.10)$$

where $\Sigma \approx 3.175911535625$ is a three-dimensional hypercubic lattice integral which can be expressed as $\Sigma = (\sqrt{3} - 1)\Gamma^2[\frac{1}{24}]\Gamma^2[\frac{11}{24}]/48\pi^2$ [26]³; ζ , δ , ρ , κ_1 , κ_4 are further lattice integrals which are only known numerically [22]; and $\bar{\mu} \equiv g_3^2$. This bare mass parameter guarantees the existence of a continuum limit for any fixed $m_3^2(\bar{\mu})$ (but $\mathcal{O}(a)$ discretization effects remain [24]).

The derivative of the vacuum energy density, f_a , with respect to the mass parameter (bare or renormalized) yields then the quadratic condensate in lattice regularization,

$$\partial_{m_3^2} f_a = \left\langle \text{Tr} [A_0^2] \right\rangle_a. \quad (3.11)$$

This can be related to the $\overline{\text{MS}}$ condensate by [21, 22]

$$\begin{aligned} \left\langle \text{Tr} [A_0^2/g_3^2] \right\rangle_{\overline{\text{MS}}} &= \\ \lim_{\beta \rightarrow \infty} \left\{ \left\langle \text{Tr} [A_0^2/g_3^2] \right\rangle_a - \left[\frac{d_A \Sigma \beta}{16\pi C_A} + \frac{d_A C_A}{(4\pi)^2} \left(\ln \beta + \zeta + \frac{\Sigma^2}{4} - \delta - \ln \frac{C_A \bar{\mu}}{3g_3^2} \right) \right] \right\}. \end{aligned} \quad (3.12)$$

Writing the renormalised mass parameter in lattice units as

$$\hat{m} \equiv a m_3(\bar{\mu} = g_3^2) = \frac{2C_A y^{\frac{1}{2}}}{\beta} \Leftrightarrow y^{\frac{1}{2}} = \frac{\beta \hat{m}}{2C_A}, \quad (3.13)$$

where y was defined in Eq. (3.5), we can express the lattice condensate as

$$\frac{1}{d_A} \left\langle \text{Tr} [A_0^2/g_3^2] \right\rangle_a = \frac{1}{d_A g_3^2} \partial_{m_3^2} f_a \quad (3.14)$$

³We thank D. Broadhurst for bringing these references to our attention.

$$\begin{aligned}
&\equiv \left(\frac{\beta\hat{m}}{2C_A}\right)^{+1} \phi_{00}(\hat{m}) + \\
&+ \left(\frac{\beta\hat{m}}{2C_A}\right)^0 \left\{ \phi_{10}(\hat{m}) + x \phi_{11}(\hat{m}) \right\} + \\
&+ \left(\frac{\beta\hat{m}}{2C_A}\right)^{-1} \left\{ \phi_{20}(\hat{m}) + \sum_{n=1}^2 x^n \left[\phi_{2n}(\hat{m}) + \tilde{\phi}_{2n}(\hat{m}) \ln\left(\frac{\beta\hat{m}}{2C_A}\right) \right] \right\} + \\
&+ \left(\frac{\beta\hat{m}}{2C_A}\right)^{-2} \left\{ \phi_{30}(\hat{m}) + \sum_{n=1}^3 x^n \left[\phi_{3n}(\hat{m}) + \tilde{\phi}_{3n}(\hat{m}) \ln\left(\frac{\beta\hat{m}}{2C_A}\right) \right] \right\} + \\
&+ \mathcal{O}\left(\frac{\beta\hat{m}}{2C_A}\right)^{-3} .
\end{aligned} \tag{3.15}$$

Regarding the structure of this equation, we note that higher powers of logarithms than the terms shown do not need to be considered, as will be explained below.

Now, super-renormalizability guarantees that only a finite set among the functions ϕ_{mn} , $\tilde{\phi}_{mn}$ diverge in the continuum limit. In fact, as can be deduced from Eq. (3.12), ϕ_{00} diverges as $1/\hat{m}$ and ϕ_{10} diverges as $\ln(1/\hat{m})$, but all the others are finite in the limit $\hat{m} \rightarrow 0$ [21]. In this limit, they then agree with the corresponding $\overline{\text{MS}}$ scheme expressions, readily extracted from Eq. (3.6), after taking note of Eq. (3.13).

For $\hat{m} \neq 0$, the functions $\phi_{mn}, \tilde{\phi}_{mn}$ can be computed in lattice perturbation theory. The first one, ϕ_{00} , follows from a 1-loop computation, while ϕ_{10}, ϕ_{11} require 2-loop computations (details are given in appendix A). The functions $\tilde{\phi}_{21}, \tilde{\phi}_{22}, \tilde{\phi}_{31}, \tilde{\phi}_{32}, \tilde{\phi}_{33}$ can be deduced from the fact that $\langle \text{Tr}[A_0^2] \rangle_a$ is independent of $\bar{\mu}$; on the other hand $\phi_{00}, \phi_{10}, \phi_{11}$ have $\bar{\mu}$ -dependence, emerging through the running of the $\overline{\text{MS}}$ mass parameter according to Eq. (3.3). This dependence must cancel against explicit 3-loop and 4-loop logarithms, containing $\ln(6/a\bar{\mu})$; these logarithms arise exclusively from the mass counterterm in Eq. (3.10). Therefore, the 3-loop and 4-loop coefficients $\tilde{\phi}_{21}, \tilde{\phi}_{22}, \tilde{\phi}_{31}, \tilde{\phi}_{32}, \tilde{\phi}_{33}$ can be deduced from mass derivatives of the 1-loop and 2-loop expressions.

As far as the ‘‘genuine’’ 3-loop coefficients are concerned, we have computed explicitly only ϕ_{21}, ϕ_{22} (details are given in appendix A). These arise from graphs containing at least one quartic coupling, which means that most of them (with one exception) factorise into products of lower-order graphs.

To display the results, we use the notation of basic lattice integrals ($\hat{J}_a, \hat{I}_a, \hat{H}_a, \hat{G}_a, \hat{B}_a$) explained in appendix B. Denoting furthermore

$$\begin{aligned}
\mathcal{K}_1(\hat{m}^2) &\equiv 2 \left[\hat{I}_a(\hat{m}^2) + \hat{I}_a(0) - \frac{\Sigma}{2\pi} \right] \hat{I}'_a(\hat{m}^2) + \hat{I}_a(0) \left[1 + \hat{m}^2 \partial_{\hat{m}^2} \right] \hat{I}_a(\hat{m}^2) + \\
&+ 4 \left[1 + \hat{m}^2 \partial_{\hat{m}^2} \right] \hat{H}_a(\hat{m}^2) + \hat{G}'_a(\hat{m}^2) , \\
\mathcal{K}_2(\hat{m}^2) &\equiv \partial_{\hat{m}^2} \mathcal{K}_1(\hat{m}^2) \\
&= 2 \left[\hat{I}_a(\hat{m}^2) + \hat{I}_a(0) - \frac{\Sigma}{2\pi} \right] \hat{I}''_a(\hat{m}^2) + \hat{I}_a(0) \left[2 + \hat{m}^2 \partial_{\hat{m}^2} \right] \hat{I}'_a(\hat{m}^2) +
\end{aligned} \tag{3.16}$$

$$+ 2 \left[\hat{I}'_a(\hat{m}^2) \right]^2 + 4 \left[2 + \hat{m}^2 \partial_{\hat{m}^2} \right] \hat{H}'_a(\hat{m}^2) + \hat{G}''_a(\hat{m}^2), \quad (3.17)$$

$$\begin{aligned} \mathcal{K}_3(\hat{m}^2) &\equiv \hat{I}'_a(\hat{m}^2) \left[\left(1 + \hat{m}^2 \partial_{\hat{m}^2} \right) \hat{H}_a(\hat{m}^2) + \frac{1}{4} \hat{G}'_a(\hat{m}^2) - \frac{1}{(4\pi)^2} \left(\ln \frac{6}{\hat{m}} + \zeta + \frac{\Sigma^2}{4} - \delta \right) \right] + \\ &+ \left[\hat{I}_a(\hat{m}^2) - \frac{\Sigma}{4\pi} \right] \left[\left(2 + \hat{m}^2 \partial_{\hat{m}^2} \right) \hat{H}'_a(\hat{m}^2) + \frac{1}{4} \hat{G}''_a(\hat{m}^2) \right] + \\ &+ \frac{1}{2} \left[\hat{I}_a(\hat{m}^2) - \frac{\Sigma}{4\pi} \right] \left[\hat{I}_a(\hat{m}^2) + \left(1 + \frac{\hat{m}^2}{2} \right) \hat{I}_a(0) - \frac{\Sigma}{2\pi} \right] \hat{I}''_a(\hat{m}^2) + \\ &+ \left[\hat{I}_a(\hat{m}^2) + \frac{1}{2} \left(1 + \frac{\hat{m}^2}{2} \right) \hat{I}_a(0) - \frac{3\Sigma}{8\pi} \right] \left[\hat{I}'_a(\hat{m}^2) \right]^2 + \\ &+ \frac{3}{4} \left[\hat{I}_a(\hat{m}^2) - \frac{\Sigma}{6\pi} \right] \hat{I}_a(0) \hat{I}'_a(\hat{m}^2), \end{aligned} \quad (3.18)$$

we obtain from appendix A, as well as from the continuum values in Eq. (3.6):

$$\phi_{00} = \frac{1}{2\hat{m}} \hat{I}_a(\hat{m}^2) \quad (3.19)$$

$$\approx \frac{\Sigma}{8\pi\hat{m}} - \frac{1}{8\pi} + \mathcal{O}(\hat{m}), \quad (3.20)$$

$$\phi_{10} = \frac{1}{4} C_A \mathcal{K}_1(\hat{m}^2) \quad (3.21)$$

$$\approx \frac{C_A}{(4\pi)^2} \left[\ln \frac{3}{\hat{m}} + \zeta + \frac{\Sigma^2}{4} - \delta + \frac{1}{4} + \mathcal{O}(\hat{m}) \right], \quad (3.22)$$

$$\phi_{11} = \frac{1}{2} (d_A + 2) \left[\hat{I}_a(\hat{m}^2) - \frac{\Sigma}{4\pi} \right] \hat{I}'_a(\hat{m}^2) \quad (3.23)$$

$$\approx \frac{d_A + 2}{(4\pi)^2} \left[\frac{1}{4} + \mathcal{O}(\hat{m}) \right], \quad (3.24)$$

$$\phi_{20} \approx \frac{C_A^2}{(4\pi)^3} \left[\frac{89}{48} - \frac{11}{12} \ln 2 + \frac{\pi^2}{12} + \mathcal{O}(\hat{m}) \right], \quad (3.25)$$

$$\phi_{21} = (d_A + 2) C_A \hat{m} \mathcal{K}_3(\hat{m}^2) \quad (3.26)$$

$$\approx \frac{(d_A + 2) C_A}{(4\pi)^3} \left[\frac{1}{2} \ln 2 + \frac{3}{8} + \mathcal{O}(\hat{m}) \right], \quad (3.27)$$

$$\tilde{\phi}_{21} = -\frac{(d_A + 2) C_A}{(4\pi)^2} \hat{m} \hat{I}'_a(\hat{m}^2) \quad (3.28)$$

$$\approx \frac{(d_A + 2) C_A}{(4\pi)^3} \left[\frac{1}{2} + \mathcal{O}(\hat{m}) \right], \quad (3.29)$$

$$\begin{aligned} \phi_{22} &= (d_A + 2) \hat{m} \left[\frac{1}{(4\pi)^2} \hat{I}'_a(\hat{m}^2) \left(\ln \frac{6}{\hat{m}} + \zeta \right) - \frac{1}{4} \hat{B}'_a(\hat{m}^2) \right] + \\ &+ \frac{1}{2} (d_A + 2)^2 \hat{m} \left[\hat{I}_a(\hat{m}^2) - \frac{\Sigma}{4\pi} \right] \times \\ &\times \left\{ \left[\hat{I}'_a(\hat{m}^2) \right]^2 + \frac{1}{2} \left[\hat{I}_a(\hat{m}^2) - \frac{\Sigma}{4\pi} \right] \hat{I}''_a(\hat{m}^2) \right\} \end{aligned} \quad (3.30)$$

$$\approx \frac{d_A + 2}{(4\pi)^3} \left[\frac{1}{4} - \ln 2 - \frac{d_A + 2}{16} + \mathcal{O}(\hat{m}) \right], \quad (3.31)$$

$$\tilde{\phi}_{22} = \frac{d_A + 2}{(4\pi)^2} \hat{m} \hat{I}'_a(\hat{m}^2) \quad (3.32)$$

$$\approx \frac{d_A + 2}{(4\pi)^3} \left[-\frac{1}{2} + \mathcal{O}(\hat{m}) \right], \quad (3.33)$$

$$\phi_{30} \approx \frac{C_A^3}{(4\pi)^4} \left[\frac{43}{8} - \frac{491}{1536} \pi^2 + \mathcal{O}(\hat{m}) \right], \quad (3.34)$$

$$\phi_{31} \approx \frac{C_A^2}{(4\pi)^4} \left[\frac{5}{2} \left(1 - \frac{\pi^2}{8} \right) + (d_A + 2) \left(\ln 2 - \frac{1}{4} \right) + \mathcal{O}(\hat{m}) \right], \quad (3.35)$$

$$\tilde{\phi}_{31} = -\frac{1}{2} \frac{(d_A + 2) C_A^2}{(4\pi)^2} \hat{m}^2 \mathcal{K}_2(\hat{m}^2) \quad (3.36)$$

$$\approx \frac{(d_A + 2) C_A^2}{(4\pi)^4} \left[1 + \mathcal{O}(\hat{m}) \right], \quad (3.37)$$

$$\phi_{32} \approx \frac{(d_A + 2) C_A}{(4\pi)^4} \left[\frac{9}{4} - \frac{\pi^2}{16} - \ln 2 - \frac{d_A + 2}{4} + \mathcal{O}(\hat{m}) \right], \quad (3.38)$$

$$\begin{aligned} \tilde{\phi}_{32} &= \frac{(d_A + 2) C_A}{(4\pi)^2} \frac{1}{2} \hat{m}^2 \mathcal{K}_2(\hat{m}^2) - \\ &- \frac{(d_A + 2)^2 C_A}{(4\pi)^2} \hat{m}^2 \left\{ \left[\hat{I}'_a(\hat{m}^2) \right]^2 + \left[\hat{I}_a(\hat{m}^2) - \frac{\Sigma}{4\pi} \right] \hat{I}''_a(\hat{m}^2) \right\} \end{aligned} \quad (3.39)$$

$$\approx \frac{(d_A + 2) C_A}{(4\pi)^4} \left[-1 + \mathcal{O}(\hat{m}) \right], \quad (3.40)$$

$$\phi_{33} \approx \frac{d_A + 2}{(4\pi)^4} \left[\frac{1}{4} (d_A + 2) - \frac{\pi^2}{48} (d_A + 8) + \mathcal{O}(\hat{m}) \right], \quad (3.41)$$

$$\tilde{\phi}_{33} = \frac{(d_A + 2)^2}{(4\pi)^2} \hat{m}^2 \left\{ \left[\hat{I}'_a(\hat{m}^2) \right]^2 + \left[\hat{I}_a(\hat{m}^2) - \frac{\Sigma}{4\pi} \right] \hat{I}''_a(\hat{m}^2) \right\} \quad (3.42)$$

$$\approx \frac{(d_A + 2)^2}{(4\pi)^4} \left[0 + \mathcal{O}(\hat{m}) \right]. \quad (3.43)$$

Note that at infinite volume, $\hat{I}_a(0) = \Sigma/4\pi$, so that the functions \mathcal{K}_1 , \mathcal{K}_2 , \mathcal{K}_3 defined in Eqs. (3.16)–(3.18) can be simplified; however, in a finite volume, $\Sigma/4\pi$ appearing in the mass counterterm is kept fixed, while $\hat{I}_a(0)$, emerging from loops, gets modified (cf. appendix B).

4. Numerical Stochastic Perturbation Theory

In order to estimate numerically the coefficients ϕ_{20} , ϕ_{30} , ϕ_{31} , ϕ_{32} , ϕ_{33} , for which only the continuum values ($\hat{m} \rightarrow 0$ limits) are known exactly (cf. Eqs. (3.25), (3.34), (3.35), (3.38),

(3.41)), we find it convenient to rewrite the action in Eq. (3.7) as

$$\begin{aligned}
S_{\text{latt}} &= \beta \sum_{\mathbf{x}, i < j} \left(1 - \frac{1}{3} \text{Re Tr} [P_{ij}(\mathbf{x})] \right) - \\
&- 2 \sum_{\mathbf{x}, i} \text{Tr} [\Phi(\mathbf{x}) U_i(\mathbf{x}) \Phi(\mathbf{x} + i) U_i^\dagger(\mathbf{x})] + \\
&+ \sum_{\mathbf{x}} \left\{ \alpha(\beta, \lambda, \hat{m}) \text{Tr} [\Phi^2(\mathbf{x})] + \lambda \left(\text{Tr} [\Phi^2(\mathbf{x})] \right)^2 \right\}, \tag{4.1}
\end{aligned}$$

where $\Phi \equiv \sqrt{a} A_0$, $\lambda \equiv a \lambda_3$, $\hat{m} \equiv a m_3 (\bar{\mu} = g_3^2)$ and, for $N_c = 3$, Eq. (3.10) implies that

$$\begin{aligned}
\alpha(\beta, \lambda, \hat{m}) &= 6 \left\{ 1 + \frac{\hat{m}^2}{6} - \left(6 + \frac{5}{3} \lambda \beta \right) \frac{3.175911525625}{4\pi\beta} - \right. \\
&- \left. \frac{3}{8\pi^2\beta^2} \left[\left(10\lambda\beta - \frac{5}{9} \lambda^2 \beta^2 \right) \left(\ln \beta + 0.08849 \right) + \frac{34.768}{6} \lambda \beta + 36.130 \right] \right\}. \tag{4.2}
\end{aligned}$$

We write the expansion of the lattice condensate now as

$$\begin{aligned}
\langle \text{Tr} [\Phi^2] \rangle &= d_{00} + d_{10} \frac{1}{\beta} + d_{11} \lambda + d_{20} \frac{1}{\beta^2} + d_{21} \frac{\lambda}{\beta} + d_{22} \lambda^2 + \\
&+ d_{30} \frac{1}{\beta^3} + d_{31} \frac{\lambda}{\beta^2} + d_{32} \frac{\lambda^2}{\beta} + d_{33} \lambda^3 + O\left(\frac{\lambda^n}{\beta^{4-n}}\right). \tag{4.3}
\end{aligned}$$

The coefficients here are related to those in Eq. (3.15) through

$$d_{00} = d_A \hat{m} \phi_{00}, \tag{4.4}$$

$$d_{10} = 2d_A C_A \phi_{10}, \tag{4.5}$$

$$d_{11} = d_A \phi_{11}, \tag{4.6}$$

$$d_{20} = \frac{4d_A C_A^2}{\hat{m}} \phi_{20}, \tag{4.7}$$

$$d_{21} = \frac{2d_A C_A}{\hat{m}} \left[\phi_{21} + \tilde{\phi}_{21} \ln \left(\frac{\beta \hat{m}}{2C_A} \right) \right], \tag{4.8}$$

$$d_{22} = \frac{d_A}{\hat{m}} \left[\phi_{22} + \tilde{\phi}_{22} \ln \left(\frac{\beta \hat{m}}{2C_A} \right) \right], \tag{4.9}$$

$$d_{30} = \frac{8d_A C_A^3}{\hat{m}^2} \phi_{30}, \tag{4.10}$$

$$d_{31} = \frac{4d_A C_A^2}{\hat{m}^2} \left[\phi_{31} + \tilde{\phi}_{31} \ln \left(\frac{\beta \hat{m}}{2C_A} \right) \right], \tag{4.11}$$

$$d_{32} = \frac{2d_A C_A}{\hat{m}^2} \left[\phi_{32} + \tilde{\phi}_{32} \ln \left(\frac{\beta \hat{m}}{2C_A} \right) \right], \tag{4.12}$$

$$d_{33} = \frac{d_A}{\hat{m}^2} \left[\phi_{33} + \tilde{\phi}_{33} \ln \left(\frac{\beta \hat{m}}{2C_A} \right) \right]. \tag{4.13}$$

The perturbative study is concretely carried out by means of *Numerical Stochastic Perturbation Theory (NSPT)* [27, 28]. (It would certainly also be interesting to pursue the same computation with standard techniques [29]; we comment on this in more detail in Sec. 6.) Its origins lie in Stochastic Quantization [30], based on introducing an extra coordinate t and an evolution equation of the Langevin type, namely

$$\partial_t \Phi(\mathbf{x}, t) = -\delta_\Phi S[\Phi] + \eta(\mathbf{x}, t), \quad (4.14)$$

where $\eta(\mathbf{x}, t)$ is a Gaussian noise. The usual Feynman-Gibbs path integral is recovered by averaging over the stochastic time,

$$Z^{-1} \int \mathcal{D}\Phi O[\Phi(\mathbf{x})] e^{-S[\Phi(\mathbf{x})]} = \lim_{t \rightarrow \infty} \frac{1}{t} \int_0^t dt' \langle O[\Phi_\eta(\mathbf{x}, t')] \rangle_\eta. \quad (4.15)$$

In the case of gauge degrees of freedom the Langevin equation reads

$$\partial_{\tilde{t}} U_{\tilde{\eta}} = -i \left(\nabla S[U_{\tilde{\eta}}] + \tilde{\eta} \right) U_{\tilde{\eta}}, \quad (4.16)$$

where $\tilde{\eta}(\mathbf{x}, \tilde{t})$ is another Gaussian noise, and \tilde{t} is another fictitious time coordinate. Both time coordinates are dimensionless, being effectively measured in spatial lattice units.

In practice, the time coordinates t, \tilde{t} need to be discretized as well: $t = n\epsilon, \tilde{t} = n\tilde{\epsilon}, n \in \mathbb{Z}$, with $\epsilon, \tilde{\epsilon} \rightarrow 0$ in the end. The discretized version of the scalar evolution, Eq. (4.14), reads

$$\Phi(\mathbf{x}, (n+1)\epsilon) = \Phi(\mathbf{x}, n\epsilon) - \epsilon \delta_{\Phi(\mathbf{x})} S + \sqrt{\epsilon} \eta(\mathbf{x}, n\epsilon), \quad (4.17)$$

while the discretized version of the link evolution, Eq. (4.16), becomes

$$U_k(\mathbf{x}, (n+1)\tilde{\epsilon}) = \exp \left\{ -i \left[\tilde{\epsilon} \nabla_{k,\mathbf{x}} S + \sqrt{\tilde{\epsilon}} \tilde{\eta}_k(\mathbf{x}, n\tilde{\epsilon}) \right] \right\} U_k(\mathbf{x}, n\tilde{\epsilon}). \quad (4.18)$$

Here $\eta \equiv T^a \eta^a, \tilde{\eta}_k \equiv T^a \tilde{\eta}_k^a$; we have rescaled the noise fields by a factor $\sqrt{\epsilon}, \sqrt{\tilde{\epsilon}}$; $\nabla_{k,\mathbf{x}} \equiv T^a \nabla_{k,\mathbf{x}}^a$, where T^a are the generators of $SU(3)$, normalised as $\text{Tr}[T^a T^b] = \delta^{ab}/2$; and the covariant derivative is defined as

$$\nabla_{k,\mathbf{x}}^a S \equiv \lim_{\delta \rightarrow 0} \frac{1}{\delta} \left\{ S[e^{i\delta T^a} U_k(\mathbf{x})] - S[U_k(\mathbf{x})] \right\}. \quad (4.19)$$

To be explicit, the expressions for the functional derivatives in Eqs. (4.17), (4.18) read

$$\begin{aligned} \delta_{\Phi(\mathbf{x})} S &= - \sum_k \left[U_k(\mathbf{x}) \Phi(\mathbf{x} + k) U_k^\dagger(\mathbf{x}) + U_k^\dagger(\mathbf{x} - k) \Phi(\mathbf{x} - k) U_k(\mathbf{x} - k) \right] + \\ &+ \alpha \Phi(\mathbf{x}) + 2\lambda \Phi(\mathbf{x}) \text{Tr}[\Phi^2(\mathbf{x})], \end{aligned} \quad (4.20)$$

$$\begin{aligned} i \nabla_{k,\mathbf{x}} S &= \frac{\beta}{12} \sum_{|l| \neq k} \left\{ P_{kl}(\mathbf{x}) - P_{kl}^\dagger(\mathbf{x}) - \frac{\mathbb{1}}{3} \text{Tr} \left[P_{kl}(\mathbf{x}) - P_{kl}^\dagger(\mathbf{x}) \right] \right\} + \\ &+ \left[U_k(\mathbf{x}) \Phi(\mathbf{x} + k) U_k^\dagger(\mathbf{x}), \Phi(\mathbf{x}) \right]. \end{aligned} \quad (4.21)$$

am_3	$\ln \beta$	N	τ
0.25	$\ln 24$	11 – 22	5 ^(a) , 10, 15, 20, 25
0.30	$\ln 24$	10 – 19	5 ^(b) , 10, 15, 20, 25
0.40	$\ln 24$	7 – 16	5 ^(c) , 10, 15, 20, 25
0.50	$\ln 24$	7 – 16	10, 15, 20, 25
0.60	$\ln 24$	10 – 15	10, 15, 20, 25
0.80	$\ln 24$	4 – 15	10, 15, 20, 25
1.00	$\ln 24$	5 – 13	10, 15, 20, 25
1.00*	$\ln 80$	10 – 13	10, 15, 20, 25

Table 1: The masses $am_3 \equiv am_3(\bar{\mu} = g_3^2)$, counter term parts $\ln \beta$ (cf. Eq. (4.2)), box sizes N ($V = a^3 N^3$), and time discretizations τ studied. The box sizes were increased in unit steps within the intervals shown. The time step $\tau = 5$ was only used for the box sizes (a) $N = 16, 19, 22$; (b) $N = 16, 19$; (c) $N = 16$. In total, our sample consists of 298 lattices.

Furthermore we write the gauge-field time-step in the form $\tilde{\epsilon} \equiv 10^{-3} \tau / \beta$, while $\epsilon \equiv 10^{-3} \tau$.

To now introduce NSPT, we expand the variables as

$$\Phi(\mathbf{x}) \longrightarrow \sum_i g_0^i \Phi^{(i)}(\mathbf{x}), \quad U_k(\mathbf{x}) = \mathbb{1} + \sum_{i=1} \beta^{-\frac{i}{2}} U_k^{(i)}(\mathbf{x}), \quad (4.22)$$

where g_0 is some small coupling; in our case, this role is played by two expansion parameters, $\beta^{-1/2}$ and λ . This results in a hierarchical system of difference equations that can be numerically solved, to obtain the series in Eq. (4.3) for $\langle \text{Tr} [\Phi^2] \rangle$, for each τ . Subsequently, we need to extrapolate to $\tau = 0$.

Finally, we recall that the gauge field equation of motion possesses a zero-mode solution. When constructing the gauge field propagator, we omit this contribution; its effects are, in any case, insignificant in the infinite-volume limit needed for constructing Eq. (4.3).

5. Data analysis

Our approach involves three different extrapolations / interpolations in total: first, the above-mentioned extrapolation to $\tau \rightarrow 0$; second, an extrapolation to infinite volume ($N \rightarrow \infty$); third, an interpolation between the different $\hat{m} = am_3(\bar{\mu} = g_3^2)$ simulated. We discuss these steps one by one. The complete data sample is listed in Table 1.

5.1. Extrapolation $\tau \rightarrow 0$

Examples of the $\tau \rightarrow 0$ extrapolations are shown in Fig. 1, at $am_3 = 0.25$, $N = 22$. (We omit, for layout-reasons, the simplest coefficient d_{00} .) The data immediately lead to the important

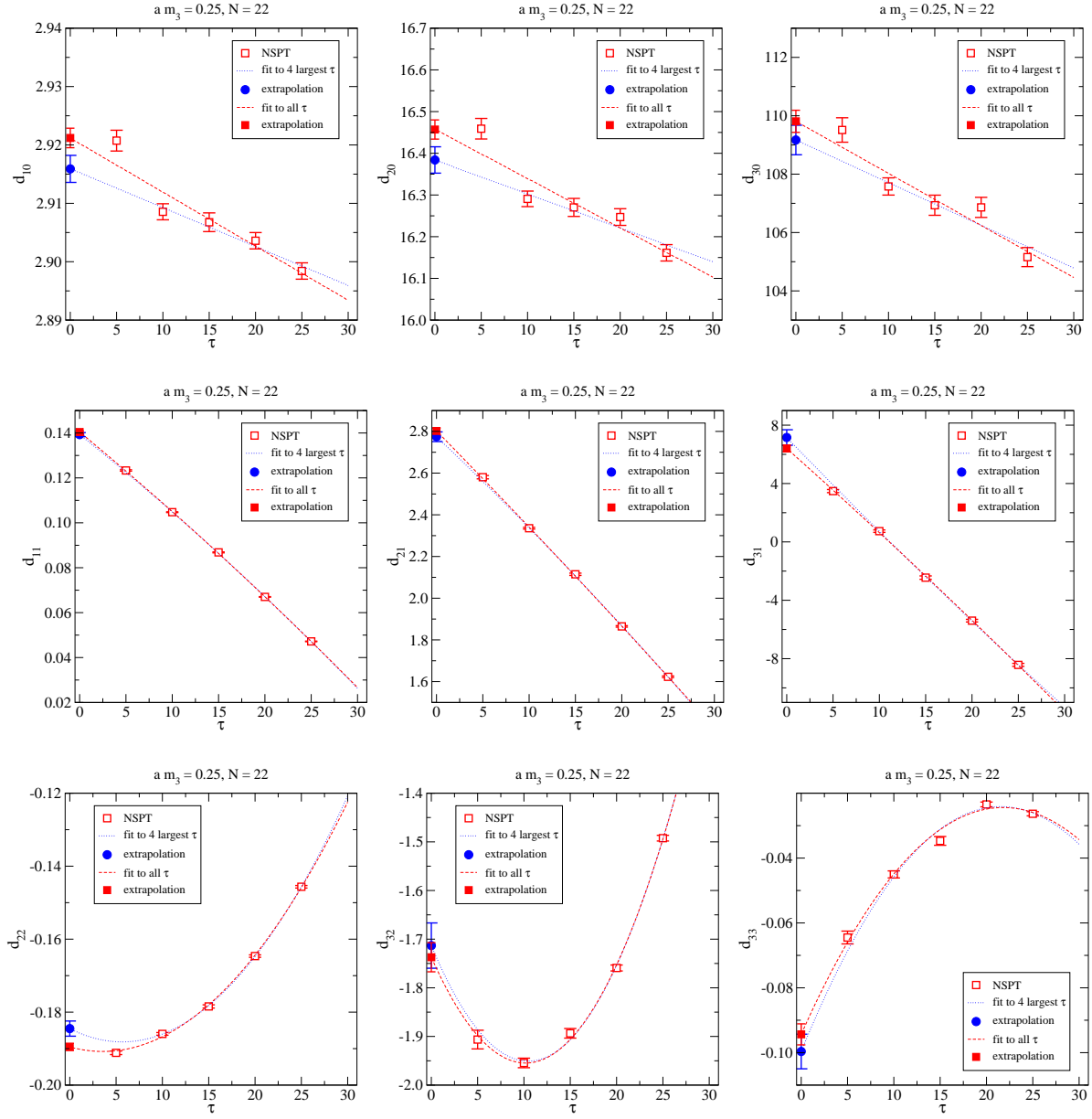


Figure 1: The results for d_{ij} as a function of τ , at $am_3 = 0.25$, $N = 22$. The curves show the results of linear or quadratic fits.

observation that the shapes of the curves are practically the same for d_{10} , d_{20} and d_{30} ; for d_{11} , d_{21} and d_{31} ; and for d_{22} and d_{32} . In other words, the behaviour as a function of τ is dictated by the number of scalar couplings λ that are associated with the coefficient. (This is at least partly due to the simple way in which we chose the time steps related to gauge and scalar field time evolutions; with some tuning, it might have been possible to optimise the time steps such that the time evolutions would have been more balanced [31].)

We have used the data at $\tau = 5$, which were the most expensive ones to produce and are only available for a subset of the parameter values, as a probe for the type of extrapolation that should be used for obtaining the $\tau \rightarrow 0$ limits. Indeed, we choose the order of the polynomial fit in τ low enough so that the results remain more or less stable in the inclusion of the $\tau = 5$ points. For d_{10} , d_{20} and d_{30} , this requires linear extrapolations; for the other coefficients, we use quadratic fits. Nevertheless, we note that in some cases the results of the extrapolations do change by a statistically significant amount in the inclusion of the points with $\tau = 5$, indicating that our systematic errors may be non-negligible.

Given the possible existence of systematic errors, it is important to crosscheck the results in a number of known cases. As has been discussed in Sec. 3, we do have exact results available, for any given am_3 and box size N , for the coefficients $d_{00}, d_{10}, d_{11}, d_{21}, d_{22}$. In Figs. 2, 3 we compare the $\tau \rightarrow 0$ extrapolations, based on 4 τ 's in most cases, and on 5 τ 's where available, with the exact values.

We observe that, in general, the results of the $\tau \rightarrow 0$ extrapolations *do* scatter around the correct values. The exception is d_{10} , and to a lesser extent d_{21} , at small volumes. We suspect that the reason for this is related to the way in which the zero-modes are subtracted in standard lattice perturbation theory (i.e. “exact values”, cf. appendix B) and in NSPT, respectively. Nevertheless, given that the discrepancy rapidly disappears with increasing volume, there does not appear to be serious reason for concern.

Moreover, we note that the extrapolations including $\tau = 5$ are in general closer to the exact values than those excluding it. In a few cases, the correct value is between the extrapolations based of 4 and 5 τ 's; in other words, the data point at $\tau = 5$ “overcorrects” the result of the extrapolation. Based on these tests, we have decided to always include extrapolations based on 4 and, where available, 5 τ 's, as independent estimates of the intercepts at $\tau = 0$. The extrapolations based on 5 τ 's have smaller error bars, and thus more weight in the subsequent fits; at the same time, the inclusion of the extrapolations based on 4 τ 's allows us to correct for the mentioned overshooting in the cases where it does take place.

5.2. Extrapolation $N \rightarrow \infty$

Given the results of the $\tau \rightarrow 0$ extrapolations (the complete data set, apart from d_{00} , is shown in Fig. 4), the next step is to extrapolate to infinite volume.

As Fig. 4 shows, finite-volume effects become small at large volumes. However, the box size $N = L/a$ required for this grows as the mass am_3 decreases (the behaviour is more or

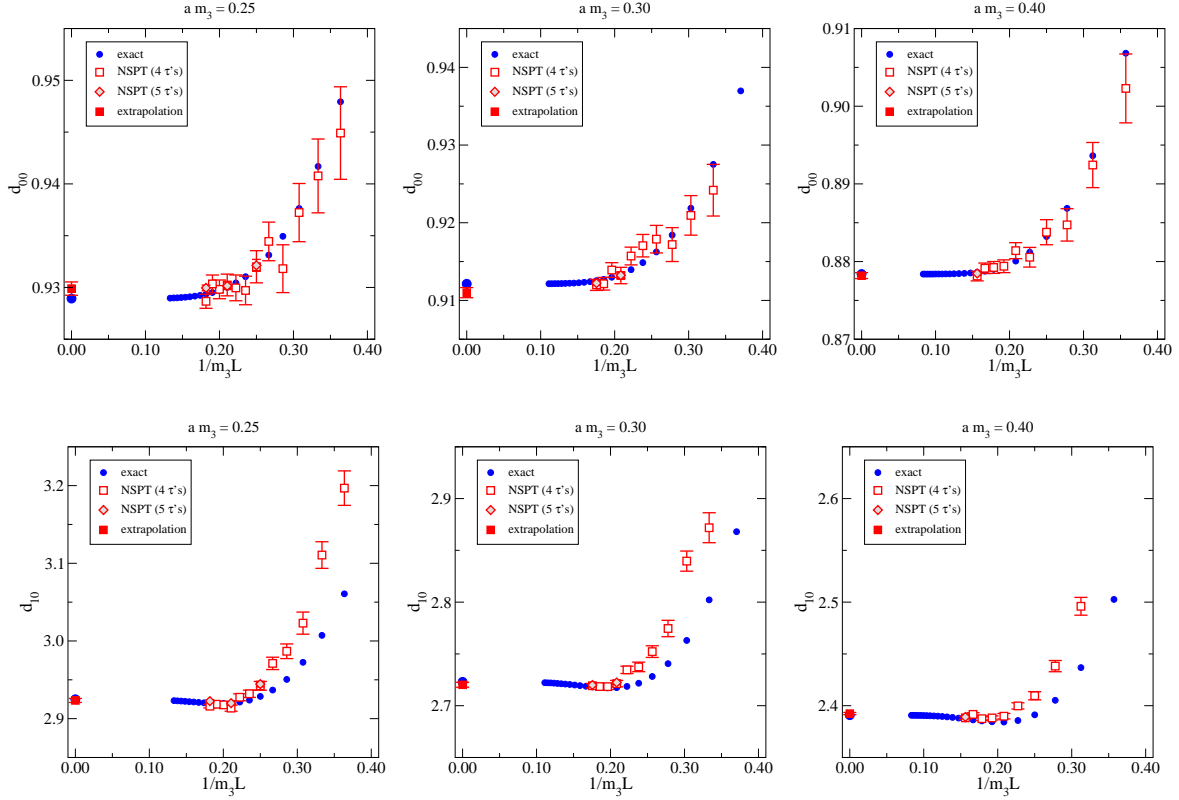


Figure 2: The results for d_{00} and d_{10} after the $\tau \rightarrow 0$ extrapolation, as a function of the inverse box size in “physical” units ($m_3L = am_3N$), together with the exact values. The (infinite volume) “extrapolation” denoted with the closed square refers to the procedure defined around Eq. (5.3).

less universal as a function of m_3L). In addition, some of the coefficients appear to require larger volumes than others. For the smallest masses, in particular, we are in many cases not yet in a region where all volume dependence has died out.

To be able to deal with this situation, some theoretical knowledge about the functional dependence on the finite volume is needed. The situation is complicated by the fact that there are both massless and massive fields in the system; therefore both powerlike and exponential volume dependences appear. However, an inspection of the known cases (Figs. 2, 3) suggests that in practice the magnitude of the power corrections is much smaller than that of the exponential ones so that, strangely enough, the latter dominate in the volumes where our data lies. In this situation, we could then expect the dominant volume behaviour to be some exponential, $d_{ij}(m_3L) - d_{ij}(\infty) \sim \exp(-m_3L)/(m_3L)^\alpha$. Unfortunately, an inspection of some of the known cases (particularly d_{22}) shows that, again because of the fairly small volumes reached in practice, the behaviour is not given by a simple exponential, but that there are

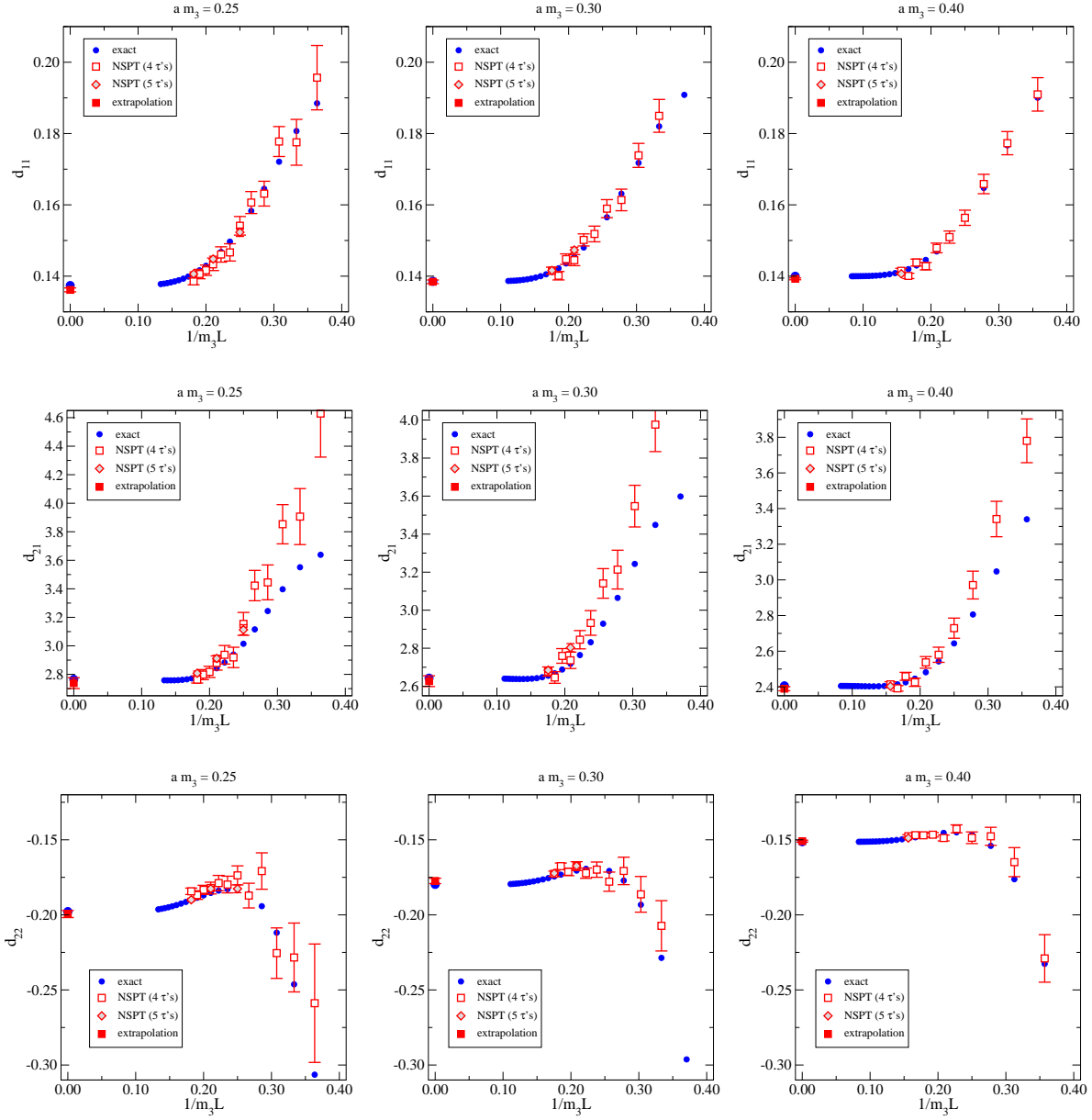


Figure 3: Like Fig. 2 but for d_{11} , d_{21} , d_{22} .

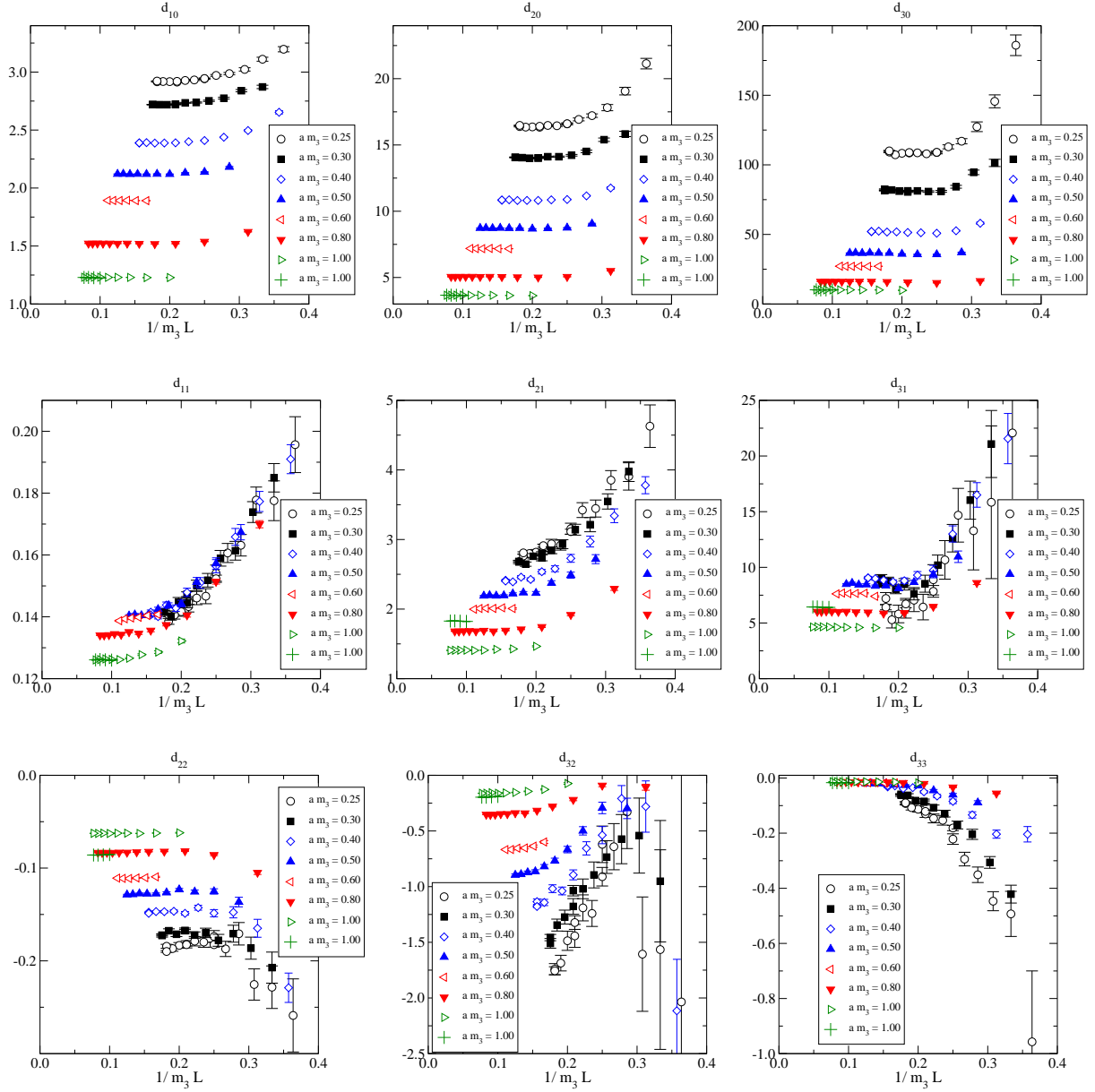


Figure 4: Shown are the $\tau \rightarrow 0$ limits for the coefficients d_{ij} , as a function of the inverse box size in “physical” units ($m_3 L = a m_3 N$). The data for $a m_3 = 1.0$ indicated with the pluses (+) is with $\ln \beta = \ln 80$; the other cases are with $\ln \beta = \ln 24$.

at least two competing universal functions, because the position of the maximum in m_3L evolves slightly with am_3 . At the same, allowing for too many free functional forms in the fits does not lead to good results either, because a long extrapolation is needed, so that the ansatz needs to be fairly constrained.

Having tested many procedures in the cases where exact results are available, we have finally chosen the following strategy in order to deal with these challenges. Let us consider a mass like $am_3 = 0.8$. Fig. 4 shows that this one has a reasonable plateau at affordable $N \leq 15$ for all the coefficients d_{ij} , but still the behaviour of the data is not too flat (i.e., some volume dependence is detectable). One can then extract an infinite-volume value $d_{ij}(\infty)$ by fitting a constant to data in the range of the plateau, and subtract it from the data in order to obtain the quantities

$$g_{ij}(m_3L) \equiv d_{ij}(m_3L) - d_{ij}(\infty) . \quad (5.1)$$

Subsequently, one can try to obtain a reasonable interpolating fit $f_{ij}(m_3L)$ for $g_{ij}(m_3L)$, allowing to go also to other values of m_3L than those simulated at $am_3 = 0.8$. In practice, we find that in the range $m_3L > 2.5$ that we have considered (cf. Table 1), our data for $am_3 = 0.8$ can be well modelled, for instance, by the ansatz

$$f_{ij}(x) \equiv e^{-x} \left[\gamma_{ij}^{(1)} + \gamma_{ij}^{(2)} \frac{1}{x} + \gamma_{ij}^{(3)} \frac{1}{x^2} \right] , \quad x = m_3L , \quad (5.2)$$

where $\gamma_{ij}^{(n)}$ are fit parameters. We have also experimented with other ansätze, but do not find a significant effect on our final results.

After this empirical determination of the finite-volume effects in one well-controlled case, we can go back to the other masses am'_3 , and use the fits f_{ij} as a constrained ansatz. However, as already mentioned, there are cases, such as d_{22} , where the position of the maximum evolves with am_3 ; therefore the results cannot be described by one universal function in our modest volumes. To incorporate this fact, we allow Eq. (5.2) to in general split up into two functions, and take a finite-size scaling ansatz of the form

$$d_{ij}(x') = d_{ij}(\infty) + A_{ij}(am'_3) \times e^{-x'} \left[\gamma_{ij}^{(1)} \right] + B_{ij}(am'_3) \times e^{-x'} \left[\gamma_{ij}^{(2)} \frac{1}{x'} + \gamma_{ij}^{(3)} \frac{1}{(x')^2} \right] , \quad (5.3)$$

where $x' \equiv m'_3L$; $d_{ij}(x')$ are the direct measurements at the mass am'_3 for various $N = L/a$; and $d_{ij}(\infty)$, $A_{ij}(am'_3)$ and $B_{ij}(am'_3)$ are volume-independent fit coefficients. Among the exactly known coefficients, the only case where the results change significantly while going from Eq. (5.2) to the more general Eq. (5.3) is precisely $d_{22}(\infty)$; among the unknown ones, the ansatz does systematically affect also $d_{20}(\infty)$, and particularly $d_{30}(\infty)$, at the smallest masses. For instance, in the last case, the values of $d_{30}(\infty)$ would be as much as $\sim 10\sigma$ higher at the two smallest masses if we employed Eq. (5.2) throughout. In the following, we cite results based on Eq. (5.3), for reasons now to be explained.

In Figs. 2, 3, the results of such fits are compared with the exact results at the smallest masses. We do find compatibility within statistical errors ($\sim 2\sigma$) in all cases. The

results for the coefficients $d_{ij} \equiv d_{ij}(\infty)$, both fitted and exact, are given in Table 2 for all masses. Only one “failure” can be detected, namely the coefficient d_{10} at the largest masses $am_3 = 0.80, 1.00$, where our (very small) NSPT error bars appear to be underestimated (the difference is $\sim 10\sigma$). Given that the largest masses are the least important ones for the subsequent steps, we have decided to let this problem “pass”; let us stress, in any case, that the overall excellent agreement is a very non-trivial result, as a long extrapolation needs to be carried out, and could only be achieved after a considerable amount of experimenting with various procedures.

Encouraged by these tests, as well as by the indication in Figs. 1, 4 that d_{20} , d_{30} could more or less behave like d_{10} ; d_{31} like d_{21} and d_{11} ; and d_{32} like d_{22} ; we then apply the same procedure to the remaining coefficients. The results are given in the lower-most panel in Table 2 (errors are statistical only). Finally, all the results, but with the normalization of Sec. 3, are shown in Fig. 5 (the exactly known values of $\tilde{\phi}_{21}$, $\tilde{\phi}_{22}$, $\tilde{\phi}_{31}$, $\tilde{\phi}_{32}$, $\tilde{\phi}_{33}$ have been used as input to convert d_{21} , d_{22} , d_{31} , d_{32} , d_{33} to ϕ_{21} , ϕ_{22} , ϕ_{31} , ϕ_{32} , ϕ_{33} , respectively; cf. Eqs. (4.8)–(4.13). The functions $\tilde{\phi}_{21}$, $\tilde{\phi}_{22}$, $\tilde{\phi}_{31}$, $\tilde{\phi}_{32}$, $\tilde{\phi}_{33}$ have been numerically crosschecked only at $am_3 = 1.00$, where simulations with two different $\ln\beta$ were carried out; cf. Table 1).

5.3. Interpolation in am_3

The remaining task is to provide interpolating fits for our functions $\phi_{ij}(am_3)$, $\tilde{\phi}_{ij}(am_3)$. Indeed, lattice simulations such as those in ref. [12] correspond to values of am_3 , given by Eq. (3.13), as well as lattice spacings $\ln\beta$, which are in the range of our study, but seldom coincide exactly with our values. The purpose of the interpolating fits is to nevertheless make our results usable for the analysis of lattice simulations.

In order to carry out the interpolating fits, a fit ansatz is again needed. Since the continuum limit corresponds to $am_3 \rightarrow 0$, it may be reasonable to use a finite-order polynomial in am_3 for this purpose. However, individual graphs do lead to other structures as well, particularly logarithms like $am_3 \ln(1/am_3)$ (cf. Eqs. (B.9), (B.12)). Even though these logarithms cancel in all the analytically known terms, we are not aware of a proof excluding them in general. In particular, the lattice simulations of ref. [12] strongly suggest the presence of such a logarithm, affecting the approach to the continuum limit, and it would then be natural for it to appear in the coefficient ϕ_{20} , which is numerically the most important unknown ingredient entering the analysis of ref. [12].

Given these considerations, we have carried out fits of two types. Defining

$$\phi_{00} = \frac{\Sigma}{8\pi am_3} + \phi_{00}^r, \quad (5.4)$$

$$\phi_{10} = \frac{C_A}{(4\pi)^2} \ln \frac{1}{am_3} + \phi_{10}^r, \quad (5.5)$$

$$\phi_{ij} = \phi_{ij}^r, \quad (ij) \neq (00), (10), \quad (5.6)$$

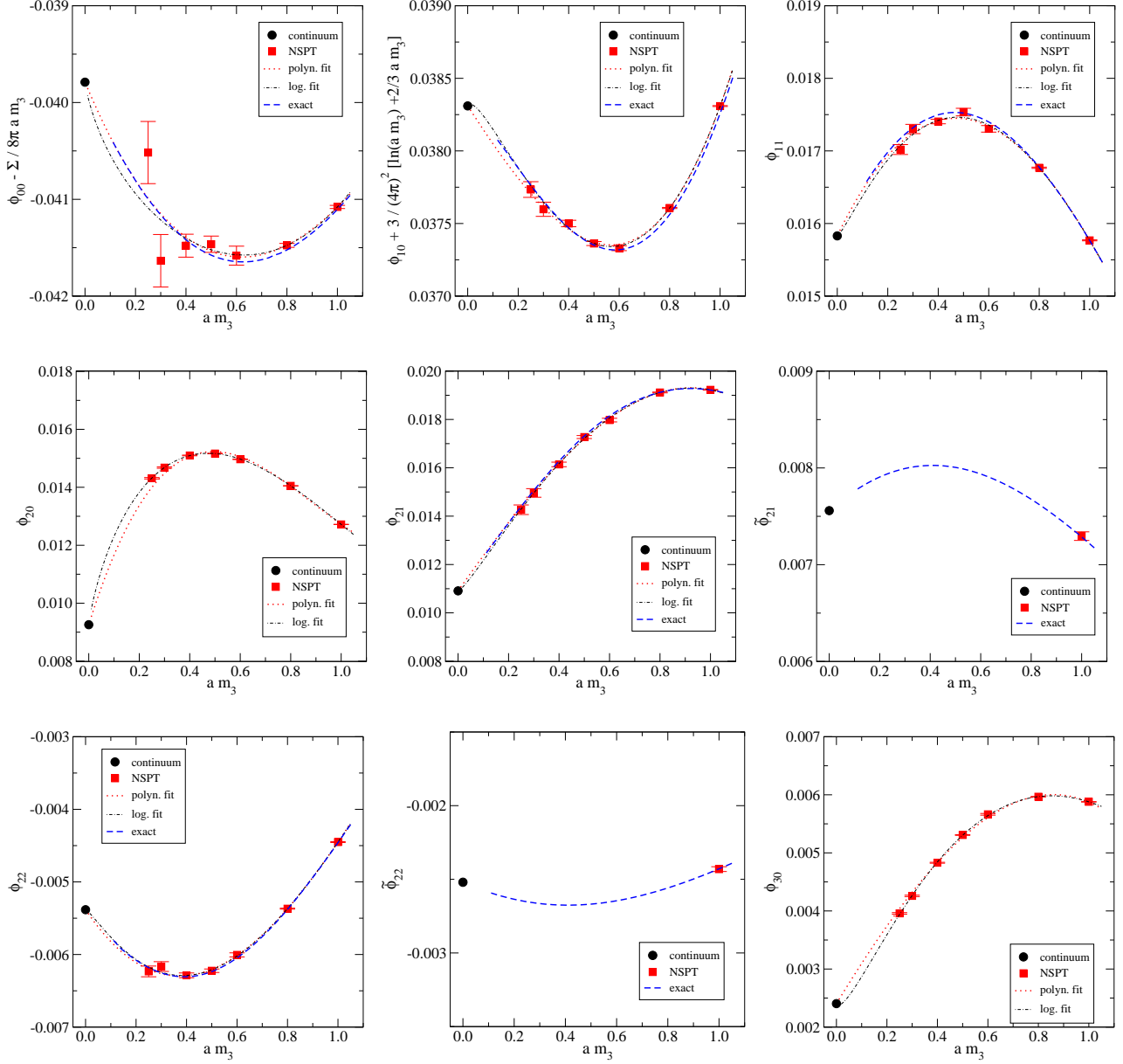


Figure 5: Shown are the coefficients in Eq. (3.15), as a function of am_3 . The polynomial fits are of third order in am_3 , and have been constrained to go through the continuum points; the logarithmic fits include the additional term $am_3 \ln(1/am_3)$, cf. Eq. (5.8).

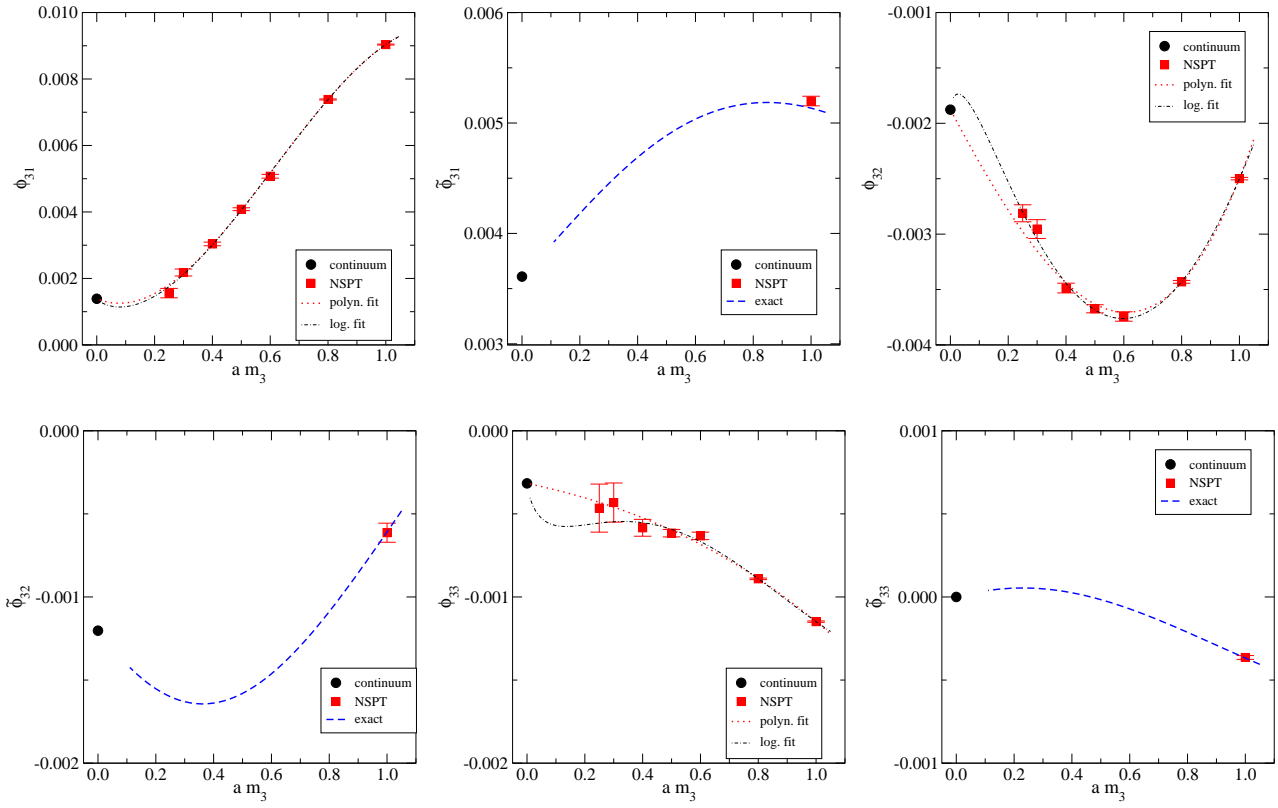


Figure 5: (Continued).

we have considered a polynomial fit,

$$\phi_{ij}^r(am_3) = a_{ij}^{(0)} + a_{ij}^{(1)} \times am_3 + a_{ij}^{(2)} \times (am_3)^2 + a_{ij}^{(3)} \times (am_3)^3, \quad (5.7)$$

and a logarithmic one,

$$\phi_{ij}^r(am_3) = b_{ij}^{(0)} + b_{ij}^{(1')} \times am_3 \ln \frac{1}{am_3} + b_{ij}^{(1)} \times am_3 + b_{ij}^{(2)} \times (am_3)^2 + b_{ij}^{(3)} \times (am_3)^3. \quad (5.8)$$

The fits have been constrained to have the correct continuum values $a_{ij}(0)$, $b_{ij}(0)$ which are known in all cases (cf. Sec. 3). The fit functions are illustrated in Fig. 5, and the results for the coefficients are given in Tables 3, 4.

Two main observations can be made from the fits:

- In all cases where exact results are available, the logarithmic fits agree reasonably well with the polynomial ones. This is expected in the sense that we know that no logarithms exist in the exactly known functions.
- For the most important unknown function, ϕ_{20} , the logarithmic fit *does* appear to produce a markedly better description of our data than a polynomial fit; $\chi^2/\text{d.o.f.}$ decreases dramatically, from ~ 55 to ~ 0.13 . (This is the case also for the second-most important unknown, ϕ_{30} , where $\chi^2/\text{d.o.f.}$ decreases from ~ 20 to ~ 1.2 .) This observation would appear to be in accordance with the indications from lattice simulations [12]. In fact, the authors in ref. [12] estimated the logarithmic term to be $\langle \text{Tr} [A_0^2/g_3^2] \rangle_a \simeq \dots + (0.10 \dots 0.13) \times g_3^2 a \ln(1/a)$, which in our units converts to $b_{20}^{(1')} \simeq (0.10 \dots 0.13)/d_A = 0.012 \dots 0.017$. Though the agreement with our value, $b_{20}^{(1')} \approx 0.00973$, is not perfect, the order of magnitude is the same. It would be interesting to re-analyze the results of ref. [12] with the coefficient of the logarithm fixed to our value.

In summary, then, there appear to be good reasons to expect the presence of logarithms in ϕ_{20} and ϕ_{30} . To unambiguously confirm this expectation, it would obviously be very interesting to find a way to improve on the accuracy of the determination of these coefficients, controlling in particular the difficult-to-estimate systematic errors that are related to the $\tau \rightarrow 0$ and $N \rightarrow \infty$ extrapolations in the present method. It would also be important to improve on the values of the coefficients associated with scalar self-couplings, ϕ_{31} , ϕ_{32} , ϕ_{33} , although this would mostly serve as a theoretical consistency check, given that the values of λ_3/g_3^2 corresponding to physical finite-temperature QCD are very small [16].

6. Conclusions

The purpose of this paper has been to estimate the (Debye) mass dependent part of the vacuum energy density of the three-dimensional SU(3) + adjoint Higgs theory, up to 4-loop order in lattice perturbation theory. The result can be parametrized in terms of the

coefficients ϕ_{ij} , $\tilde{\phi}_{ij}$, defined in Eq. (3.15). We have worked out the expressions for a number of these coefficients analytically (Eqs. (3.19)–(3.42)), and estimated the remaining ones, ϕ_{20} , ϕ_{30} , ϕ_{31} , ϕ_{32} , ϕ_{33} , for which only the continuum values are known analytically, with the help of Numerical Stochastic Perturbation Theory. The results are illustrated in Fig. 5, and parametrized in terms of simple fits in Eqs. (5.7), (5.8).

The main practical use of our results is that when combined with lattice Monte Carlo data, they should allow to improve on the analysis of the sum (beyond the known 4-loop order) of infrared sensitive contributions to the pressure [25] and quark number susceptibilities [12] of hot QCD, given that discretization errors up to the 4-loop order can now be subtracted. However, our results might also have some theoretical interest beyond these particular applications. For instance, they serve as a consistency check of the 4-loop $\overline{\text{MS}}$ -scheme computation of ref. [23] (in the sense that our results appear to be consistent with the continuum values indicated in Fig. 5), as well as of the super-renormalizability of the theory considered and the power-counting arguments presented for it in ref. [21] (in the sense that no indications of ultraviolet divergences apart from the known 1-loop and 2-loop ones in ϕ_{00} , ϕ_{10} were seen).

Concerning the new coefficients ϕ_{20} , ϕ_{30} , ϕ_{31} , ϕ_{32} and ϕ_{33} , we unfortunately have to acknowledge that it appears difficult to improve significantly on the accuracy of our results with the present techniques. The problem is that two different extrapolations, $\tau \rightarrow 0$ and $N \rightarrow \infty$, are needed in order to obtain the values at any fixed am_3 , and both of these extrapolations introduce systematic and statistical errors. Therefore there is a need to crosscheck our results, and improve upon them, with standard techniques [29]. Nevertheless, even in that approach, our study should serve as a basic framework. In particular, we would like to stress the insight that it is valuable to determine the coefficients ϕ_{ij} , $\tilde{\phi}_{ij}$ as functions of am_3 , rather than to carry out an expansion in small am_3 , since realistic values of am_3 ($\sim 0.1 \dots 0.5$ [12]) are in a region where the functions show more structure than just linear terms (cf. Fig. 5). The most important coefficients to determine are ϕ_{20} and ϕ_{30} , which are independent of the scalar self-coupling, and for $am_3 \ll 1$, a concrete challenge is to confirm or disprove the existence of the logarithmic term $\sim \mathcal{O}(a \ln(1/a))$ in ϕ_{20} , for which independent indications have been seen in ref. [12] and in the present study.

Acknowledgments

We thank V. Miccio for collaboration at preliminary stages of this work, and A. Hietanen and K. Rummukainen for useful discussions. The Parma group acknowledges support from I.N.F.N. under contract *i.s. MI11*. We warmly thank *ECT**, *Trento*, for providing computing time on the *BEN* system. The total amount of computing time used for this project corresponds to about 4×10^{18} flop.

Appendix A. Graph-by-graph results for the vacuum energy density

We list here results for the mass-dependent part of the vacuum energy density f_a of the theory in Eq. (3.7) (through Eq. (3.11) this produces the condensate that we are interested in). At the 3-loop level we have only kept terms involving at least one λ_3 . In the graphical notation to be used below, solid/wiggly lines represent tree-level A_0/A_i lattice propagators, respectively.

1-loop and 2-loop graphs. For brevity, we denote in the following $m \equiv m_3(\bar{\mu})$. The integrals appearing are defined in appendix B, and in terms of these, the results read ($d = 3$):

$$\text{○} = \frac{d_A}{2} J_a(m^2), \quad (\text{A.1})$$

$$\text{○} \text{○} = \frac{\lambda_3}{4} d_A (d_A + 2) [I_a(m^2)]^2, \quad (\text{A.2})$$

$$\begin{aligned} \text{○} + \text{○} \text{○} \text{○} &= \frac{g_3^2}{4} d_A C_A \left\{ (2d - 4) I_a(0) I_a(m^2) + [I_a(m^2)]^2 + 4m^2 H_a(m^2) + \right. \\ &\quad \left. + a^2 \left[m^2 I_a(0) I_a(m^2) - I_a(0)/a^d + G_a(m^2) \right] \right\}. \end{aligned} \quad (\text{A.3})$$

3-loop graphs involving λ_3 .

$$\text{○} \text{○} \text{○} = \frac{\lambda_3^2}{4} d_A (d_A + 2)^2 [I_a(m^2)]^2 I'_a(m^2), \quad (\text{A.4})$$

$$\text{○} \text{○} = -\frac{\lambda_3^2}{4} d_A (d_A + 2) B_a(m^2), \quad (\text{A.5})$$

$$\begin{aligned} \text{○} \text{○} + \text{○} \text{○} \text{○} &= \frac{g_3^2 \lambda_3}{4} d_A C_A (d_A + 2) I_a(m^2) \left\{ (2d - 4) I_a(0) I'_a(m^2) + \right. \\ &\quad \left. + 2I_a(m^2) I'_a(m^2) + 4H_a(m^2) + 4m^2 H'_a(m^2) + \right. \\ &\quad \left. + a^2 \left[I_a(0) I_a(m^2) + m^2 I_a(0) I'_a(m^2) + G'_a(m^2) \right] \right\}, \end{aligned} \quad (\text{A.6})$$

$$\text{○} \text{○} \text{○} = 0. \quad (\text{A.7})$$

Mass counterterm contributions up to 3-loop order. Gauge field “mass counterterms” (arising from the Haar integration measure) are not displayed, as they do not contribute to terms involving at least one λ_3 .

$$\text{○} \text{✱} = \frac{d_A}{2} \delta m_a^2 I_a(m^2), \quad (\text{A.8})$$

$$\text{✱} \text{○} \text{✱} = \frac{d_A}{4} (\delta m_a^2)^2 I'_a(m^2), \quad (\text{A.9})$$

$$\text{○} \text{○} \text{✱} = \frac{\lambda_3}{2} d_A (d_A + 2) \delta m_a^2 I_a(m^2) I'_a(m^2), \quad (\text{A.10})$$

$$\text{○} \text{✱} + \text{○} \text{○} \text{○} = \frac{g_3^2}{4} d_A C_A \delta m_a^2 \left\{ (2d - 4) I_a(0) I'_a(m^2) + \right. \quad (\text{A.11})$$

$$+ 2I_a(m^2)I'_a(m^2) + 4H_a(m^2) + 4m^2H'_a(m^2) + a^2 \left[I_a(0)I_a(m^2) + m^2I_a(0)I'_a(m^2) + G'_a(m^2) \right] \}.$$

Appendix B. Basic lattice integrals

We detail here the definitions of the basic lattice integrals that appear in the expressions discussed in Sec. 3. The integration measure is

$$\int dp \equiv \int_{-\pi}^{\pi} \frac{d^3p}{(2\pi)^3}, \quad (\text{B.1})$$

and we define the standard lattice momenta as

$$\tilde{p}_i \equiv 2 \sin \frac{p_i}{2}, \quad \tilde{p}^2 \equiv \sum_{i=1}^3 \tilde{p}_i^2. \quad (\text{B.2})$$

The integrals appearing then read (we use hats as a reminder of the use of lattice units in these expressions):

$$\hat{J}_a(\hat{m}^2) \equiv \int dp \ln(\tilde{p}^2 + \hat{m}^2), \quad (\text{B.3})$$

$$\hat{I}_a(\hat{m}^2) \equiv \int dp \frac{1}{\tilde{p}^2 + \hat{m}^2}, \quad (\text{B.4})$$

$$\hat{H}_a(\hat{m}^2) \equiv \int dp dq \frac{1}{(\tilde{p}^2 + \hat{m}^2)(\tilde{q}^2 + \hat{m}^2)\widetilde{(p+q)}^2}, \quad (\text{B.5})$$

$$\hat{G}_a(\hat{m}^2) \equiv \int dp dq \frac{\sum_i \tilde{p}_i^2 \tilde{q}_i^2}{(\tilde{p}^2 + \hat{m}^2)(\tilde{q}^2 + \hat{m}^2)\widetilde{(p+q)}^2}. \quad (\text{B.6})$$

Small- \hat{m} expansions for these functions have been worked out in refs. [21, 22] and are given, to the order that was used for the small- \hat{m} expansions in Sec. 3, by

$$\hat{J}'_a(\hat{m}^2) = \hat{I}_a(\hat{m}^2), \quad (\text{B.7})$$

$$\hat{I}_a(\hat{m}^2) = \frac{1}{4\pi} \left[\Sigma - \hat{m} + \mathcal{O}(\hat{m}^2) \right], \quad (\text{B.8})$$

$$\hat{H}_a(\hat{m}^2) = \frac{1}{(4\pi)^2} \left[\ln \frac{3}{\hat{m}} + \frac{1}{2} + \zeta + \mathcal{O}(\hat{m}) \right], \quad (\text{B.9})$$

$$\hat{G}_a(\hat{m}^2) = \frac{1}{(4\pi)^2} \left[16\kappa_1 - 4\delta \hat{m}^2 + \mathcal{O}(\hat{m}^3) \right], \quad (\text{B.10})$$

where Σ , ζ , κ_1 and δ are numerical coefficients mentioned below Eq. (3.10). Furthermore, we define a 3-loop “basketball” integral through

$$\hat{B}_a(\hat{m}^2) \equiv \int dp dq dr \frac{1}{(\tilde{p}^2 + \hat{m}^2)(\tilde{q}^2 + \hat{m}^2)(\tilde{r}^2 + \hat{m}^2)\widetilde{(p+q+r)}^2 + \hat{m}^2}. \quad (\text{B.11})$$

In this case the small- \hat{m} expansion reads

$$\hat{B}_a(\hat{m}^2) = \frac{1}{(4\pi)^3} \left[\Sigma \times \theta - \hat{m} \left(4 \ln \frac{3}{2\hat{m}} + 4\zeta + 6 \right) + \mathcal{O}(\hat{m}^2) \right]. \quad (\text{B.12})$$

The derivation of this result, which has to our knowledge not appeared in the literature before, as well as a numerical estimate for the new coefficient θ , are given in appendix C.

The expressions in appendix A employ the functions

$$J_a(m^2) \equiv \frac{1}{a^3} \hat{J}_a(\hat{m}^2), \quad (\text{B.13})$$

$$I_a(m^2) \equiv \frac{1}{a} \hat{I}_a(\hat{m}^2), \quad (\text{B.14})$$

$$H_a(m^2) \equiv \hat{H}_a(\hat{m}^2), \quad (\text{B.15})$$

$$G_a(m^2) \equiv \frac{1}{a^4} \hat{G}_a(\hat{m}^2), \quad (\text{B.16})$$

$$B_a(m^2) \equiv \frac{1}{a} \hat{B}_a(\hat{m}^2), \quad (\text{B.17})$$

where a is the lattice spacing, and $\hat{m} \equiv am$.

In a finite volume, $V = (aN)^3$, the momentum integrations get replaced with

$$\int dp f(\mathbf{p}) \rightarrow \frac{1}{N^3} \sum_{n_1=0}^{N-1} \sum_{n_2=0}^{N-1} \sum_{n_3=0}^{N-1} f\left(\frac{2\pi\mathbf{n}}{N}\right), \quad (\text{B.18})$$

where $\mathbf{n} \equiv (n_1, n_2, n_3)$. In the case of massless propagators, the zero-mode is left out.

Appendix C. The 3-loop basketball in lattice regularization

In order to work out the expansion in Eq. (B.12), we find it convenient to return from lattice units to physical units, considering then the function in Eq. (B.17). Let us introduce the scalar propagator on the lattice,

$$D_a(x; m) \equiv \int_{-\pi/a}^{\pi/a} \frac{d^3p}{(2\pi)^3} \frac{e^{ip \cdot x}}{\tilde{p}^2 + m^2}, \quad (\text{C.1})$$

where now $\tilde{p}^2 \equiv \sum_{i=1}^3 \tilde{p}_i^2$, $\tilde{p}_i \equiv \frac{2}{a} \sin \frac{ap_i}{2}$. For $x \neq 0$, the propagator remains finite in the continuum limit $a \rightarrow 0$,

$$D_0(x; m) = \frac{\exp(-m|x|)}{4\pi|x|}, \quad (\text{C.2})$$

while for $x = 0$, it contains a linear divergence as shown in Eq. (B.8),

$$D_a(0; m) = \frac{1}{4\pi a} \left[\Sigma - \hat{m} + \mathcal{O}(\hat{m}^2) \right]. \quad (\text{C.3})$$

The integral we will be concerned with here is of the “basketball” type,

$$B_a^{(n)}(\{m_i\}) \equiv \sum_x a^3 \prod_{i=1}^n D_a(x; m_i). \quad (\text{C.4})$$

For $n = 3$, this equals the integral H_a defined in Eq. (B.5), and for general masses, the expansion close to the continuum limit is of the form [21]

$$B_a^{(3)}(\{m_i\}) = \frac{1}{(4\pi)^2} \left[\ln \frac{6}{a \sum_i m_i} + \frac{1}{2} + \zeta + \mathcal{O}(am_i) \right]. \quad (\text{C.5})$$

The challenge now is to find the corresponding expansion for $n = 4$.

The basic approach we follow is similar to the one used for the basketball integral in dimensional regularization in refs. [32]. The summation over configuration space in Eq. (C.4) is divided into two regions, $|x| \leq r$ and $|x| > r$. We assume $am_i \ll 1$, and can thus choose

$$a \ll r \ll \frac{1}{m_i}. \quad (\text{C.6})$$

In the region $|x| \leq r$, we now have $|x|m_i \ll 1$, and can expand in the masses; in the region $|x| > r$, we have $a/|x| \ll 1$, and can use the continuum approximation for the propagators.

The region $|x| > r$. The region of large $|x|$ gives a contribution which remains finite in the limit $a \rightarrow 0$. It can thus be evaluated employing Eq. (C.2). The integral is elementary, and we obtain

$$\begin{aligned} \lim_{a \rightarrow 0} \Delta_{|x| > r} B_a^{(4)}(\{m_i\}) &= \int_r^\infty 4\pi |x|^2 dx \prod_{i=1}^4 D_0(x; m_i) \\ &= \frac{1}{(4\pi)^3} \left[\frac{1}{r} + M \left(\ln Mr + \gamma_E - 1 \right) \right] + \mathcal{O}(M^2 r), \end{aligned} \quad (\text{C.7})$$

where $M \equiv m_1 + m_2 + m_3 + m_4$. Note in passing, for future reference, that

$$\int_r^\infty 4\pi |x|^2 dx \prod_{i=1}^3 D_0(x; m_i) = \frac{1}{(4\pi)^2} \left(-\ln \tilde{M} r - \gamma_E \right) + \mathcal{O}(\tilde{M} r), \quad (\text{C.8})$$

where $\tilde{M} \equiv m_1 + m_2 + m_3$.

The region $|x| \leq r$. In the region of small $|x|$, we rewrite the propagator of Eq. (C.1) in the equivalent form

$$D_a(x; m) = \int_{-\pi/a}^{\pi/a} \frac{d^3 p}{(2\pi)^3} \left[\frac{e^{ip \cdot x}}{\tilde{p}^2} + \frac{1}{\tilde{p}^2 + m^2} - \frac{1}{\tilde{p}^2} - m^2 \frac{e^{ip \cdot x} - 1}{\tilde{p}^2(\tilde{p}^2 + m^2)} \right]. \quad (\text{C.9})$$

The point of this rewriting is that for $a \rightarrow 0$ and $x \neq 0$, the first term behaves as $\sim 1/4\pi|x|$, the next two combine into a constant $\sim -m/4\pi$, while the last term, which is both ultraviolet

and infrared finite, behaves as $\mathcal{O}(m^2|x|)$. Therefore, if we consider the limit $a \rightarrow 0$, $rm_i \ll 1$, the last term does not contribute in $\Delta_{|x| \leq r} B_a^{(4)}(\{m_i\})$:

$$\int_0^r |x|^2 d|x| \frac{1}{(4\pi|x|)^3} \mathcal{O}(m_i^2|x|) \sim \mathcal{O}(m_i^2 r). \quad (\text{C.10})$$

The same is true for the case that there are two or more appearances of the constant term:

$$\int_0^r |x|^2 d|x| \frac{1}{(4\pi|x|)^2} \mathcal{O}(m_i) \mathcal{O}(m_j) \sim \mathcal{O}(m_i m_j r). \quad (\text{C.11})$$

Thus the only contributions come from four appearances of the first term in Eq. (C.9), and three appearances of the first term as well as one appearance of the middle terms:

$$\begin{aligned} \lim_{a \rightarrow 0} \Delta_{|x| \leq r} B_a^{(4)}(\{m_i\}) &= \lim_{a \rightarrow 0} \sum_{|x| \leq r} a^3 [D_a(x; 0)]^4 \\ &+ \lim_{a \rightarrow 0} \left\{ \sum_{i=1}^4 [D_a(0; m_i) - D_a(0, 0)] \sum_{|x| \leq r} a^3 [D_a(x; 0)]^3 \right\} + \mathcal{O}(m_i^2 r). \end{aligned} \quad (\text{C.12})$$

Here and in the following, $\lim_{a \rightarrow 0}$ is meant in a symbolic sense, since the sums actually diverge as $a \rightarrow 0$.

Given that $D_a(0; m_i) - D_a(0, 0)$ is known (cf. Eq. (C.3)), we are left with the evaluation of the sums on the first and second rows in Eq. (C.12). Since the propagators are massless, the outcomes only depend on the ratio r/a , where $a \ll r$. The first of the sums can be performed by extending the sum to be over all space, and taking the continuum limit in the resulting subtraction, which is ultraviolet finite:

$$\begin{aligned} \lim_{a \rightarrow 0} \sum_{|x| \leq r} a^3 [D_a(x; 0)]^4 &= \lim_{a \rightarrow 0} \sum_x a^3 [D_a(x; 0)]^4 - \lim_{a \rightarrow 0} \sum_{|x| > r} a^3 [D_a(x; 0)]^4 \\ &= \lim_{a \rightarrow 0} \sum_x a^3 [D_a(x; 0)]^4 - \frac{1}{(4\pi)^3} \frac{1}{r}, \end{aligned} \quad (\text{C.13})$$

where we used Eq. (C.7). The latter sum is slightly more difficult because it would be infrared divergent at large distances, but it can be performed as above, once we regulate the infrared with mass terms, and use then Eqs. (C.5), (C.8):

$$\begin{aligned} \lim_{a \rightarrow 0} \sum_{|x| \leq r} a^3 [D_a(x; 0)]^3 &= \lim_{\tilde{M} \rightarrow 0} \left\{ \lim_{a \rightarrow 0} \sum_x a^3 \prod_{i=1}^3 D_a(x; m_i) - \lim_{a \rightarrow 0} \sum_{|x| > r} a^3 \prod_{i=1}^3 D_a(x; m_i) \right\} \\ &= \lim_{a \rightarrow 0} \left\{ \frac{1}{(4\pi)^2} \left(\ln \frac{6}{a\tilde{M}} + \frac{1}{2} + \zeta + \ln \tilde{M}r + \gamma_E \right) \right\}. \end{aligned} \quad (\text{C.14})$$

The infrared regulator \tilde{M} is seen to cancel in Eq. (C.14), as it should.

Combining now Eqs. (C.3), (C.7), (C.12), (C.13) and (C.14), terms singular in r cancel, and the limit $m_i r \rightarrow 0$ can be taken. The Euler gamma-constants γ_E also cancel, and we finally obtain

$$B_a^{(4)}(\{m_i\}) = \sum_x a^3 [D_a(x;0)]^4 - \frac{M}{(4\pi)^3} \left(\ln \frac{6}{aM} + \frac{3}{2} + \zeta \right) + \mathcal{O}(am_i^2). \quad (\text{C.15})$$

The task remains to evaluate the sum in Eq. (C.15). Employing the techniques introduced in ref. [33] and worked out for the three-dimensional case in ref. [34], we find that

$$\sum_x a^3 [D_a(x;0)]^4 \equiv \frac{1}{a} \frac{\Sigma}{(4\pi)^3} \theta, \quad \theta = 3.0122(1), \quad (\text{C.16})$$

where the number in parentheses indicates the uncertainty of the last digit. Combining Eqs. (C.15), (C.16) leads to Eq. (B.12).

Finally, recall for completeness that in dimensional regularization (DR) at $d = 3 - 2\epsilon$, the 2-loop [35] and 3-loop [36] basketball integrals read ($M = \sum_{i=1}^4 m_i$, $\tilde{M} = \sum_{i=1}^3 m_i$)

$$B_{\text{DR}}^{(3)}(\{m_i\}) = \frac{\mu^{-4\epsilon}}{(4\pi)^2} \left(\frac{1}{4\epsilon} + \ln \frac{\bar{\mu}}{\tilde{M}} + \frac{1}{2} + \mathcal{O}(\epsilon) \right), \quad (\text{C.17})$$

$$B_{\text{DR}}^{(4)}(\{m_i\}) = -\frac{\mu^{-6\epsilon}}{(4\pi)^3} M \left(\frac{1}{4\epsilon} + \frac{3}{2} \ln \frac{\bar{\mu}}{M} + 2 + \frac{1}{2} \sum_{i=1}^4 \frac{m_i}{M} \ln \frac{M}{2m_i} + \mathcal{O}(\epsilon) \right). \quad (\text{C.18})$$

For a complete discussion of basketball integrals in dimensional regularization, see ref. [37].

References

- [1] P. Ginsparg, *First and second order phase transitions in gauge theories at finite temperature*, Nucl. Phys. B 170 (1980) 388; T. Appelquist and R.D. Pisarski, *High-temperature Yang-Mills theories and three-dimensional Quantum Chromodynamics*, Phys. Rev. D 23 (1981) 2305.
- [2] K. Kajantie, M. Laine, K. Rummukainen and M. Shaposhnikov, *Generic rules for high temperature dimensional reduction and their application to the Standard Model*, Nucl. Phys. B 458 (1996) 90 [hep-ph/9508379].
- [3] E. Braaten and A. Nieto, *Free energy of QCD at high temperature*, Phys. Rev. D 53 (1996) 3421 [hep-ph/9510408].
- [4] A.D. Linde, *Infrared problem in thermodynamics of the Yang-Mills gas*, Phys. Lett. B 96 (1980) 289.
- [5] D.J. Gross, R.D. Pisarski and L.G. Yaffe, *QCD and instantons at finite temperature*, Rev. Mod. Phys. 53 (1981) 43.

- [6] P. Arnold and C. Zhai, *The three loop free energy for pure gauge QCD*, Phys. Rev. D 50 (1994) 7603 [hep-ph/9408276]; *The three loop free energy for high temperature QED and QCD with fermions*, *ibid.* 51 (1995) 1906 [hep-ph/9410360].
- [7] C. Zhai and B. Kastening, *The free energy of hot gauge theories with fermions through g^5* , Phys. Rev. D 52 (1995) 7232 [hep-ph/9507380].
- [8] K. Kajantie, M. Laine, K. Rummukainen and Y. Schröder, *The pressure of hot QCD up to $g^6 \ln(1/g)$* , Phys. Rev. D 67 (2003) 105008 [hep-ph/0211321].
- [9] S. Caron-Huot and G.D. Moore, *Heavy quark diffusion in QCD and $\mathcal{N} = 4$ SYM at next-to-leading order*, JHEP 02 (2008) 081 [arXiv:0801.2173].
- [10] A. Vuorinen, *Quark number susceptibilities of hot QCD up to $g^6 \ln(g)$* , Phys. Rev. D 67 (2003) 074032 [hep-ph/0212283]; J.P. Blaizot, E. Iancu and A. Rebhan, *On the apparent convergence of perturbative QCD at high temperature*, Phys. Rev. D 68 (2003) 025011 [hep-ph/0303045]; M. Laine and M. Vepsäläinen, *Mesonic correlation lengths in high-temperature QCD*, JHEP 02 (2004) 004 [hep-ph/0311268]; M. Vepsäläinen, *Mesonic screening masses at high temperature and finite density*, JHEP 03 (2007) 022 [hep-ph/0701250]; M. Laine and Y. Schröder, *Two-loop QCD gauge coupling at high temperatures*, JHEP 03 (2005) 067 [hep-ph/0503061]; P. Giovannangeli, *Two loop renormalization of the magnetic coupling and non-perturbative sector in hot QCD*, Nucl. Phys. B 738 (2006) 23 [hep-ph/0506318]; P. de Forcrand, B. Lucini and D. Noth, *'t Hooft loops and perturbation theory*, PoS LAT2005 (2006) 323 [hep-lat/0510081]; M. Laine and Y. Schröder, *Quark mass thresholds in QCD thermodynamics*, Phys. Rev. D 73 (2006) 085009 [hep-ph/0603048].
- [11] A. Hart, M. Laine and O. Philipsen, *Static correlation lengths in QCD at high temperatures and finite densities*, Nucl. Phys. B 586 (2000) 443 [hep-ph/0004060]; A. Vuorinen, *The pressure of QCD at finite temperatures and chemical potentials*, Phys. Rev. D 68 (2003) 054017 [hep-ph/0305183].
- [12] A. Hietanen and K. Rummukainen, *Quark number susceptibility at high temperature*, PoS LAT2006 (2006) 137 [hep-lat/0610111]; *Quark number susceptibility of high temperature and finite density QCD*, PoS LAT2007 (2007) 192 [arXiv:0710.5058]; *The diagonal and off-diagonal quark number susceptibility of high temperature and finite density QCD*, JHEP 04 (2008) 078 [arXiv:0802.3979].
- [13] M. Cheng *et al.*, *The spatial string tension and dimensional reduction in QCD*, arXiv:0806.3264 [hep-lat].
- [14] F. Di Renzo, M. Laine, V. Miccio, Y. Schröder and C. Torrero, *The leading non-perturbative coefficient in the weak-coupling expansion of hot QCD pressure*, JHEP 07 (2006) 026 [hep-ph/0605042].

- [15] A. Gynther, M. Laine, Y. Schröder, C. Torrero and A. Vuorinen, *Four-loop pressure of massless $O(N)$ scalar field theory*, JHEP 04 (2007) 094 [hep-ph/0703307].
- [16] K. Kajantie, M. Laine, K. Rummukainen and M. Shaposhnikov, *3d $SU(N)$ + adjoint Higgs theory and finite-temperature QCD*, Nucl. Phys. B 503 (1997) 357 [hep-ph/9704416].
- [17] S. Chapman, *A new dimensionally reduced effective action for QCD at high temperature*, Phys. Rev. D 50 (1994) 5308 [hep-ph/9407313].
- [18] A. Hietanen, K. Kajantie, M. Laine, K. Rummukainen and Y. Schröder, *Plaquette expectation value and gluon condensate in three dimensions*, JHEP 01 (2005) 013 [hep-lat/0412008]; A. Hietanen and A. Kurkela, *Plaquette expectation value and lattice free energy of three-dimensional $SU(N_c)$ gauge theory*, JHEP 11 (2006) 060 [hep-lat/0609015].
- [19] A. Dumitru, Y. Hatta, J. Lenaghan, K. Orginos and R.D. Pisarski, *Deconfining phase transition as a matrix model of renormalized Polyakov loops*, Phys. Rev. D 70 (2004) 034511 [hep-th/0311223]; P. Bialas, A. Morel and B. Petersson, *A gauge theory of Wilson lines as a dimensionally reduced model of QCD_3* , Nucl. Phys. B 704 (2005) 208 [hep-lat/0403027]; E. Megías, E. Ruiz Arriola and L.L. Salcedo, *Dimension two condensates and the Polyakov loop above the deconfinement phase transition*, JHEP 01 (2006) 073 [hep-ph/0505215]; R.D. Pisarski, *Effective theory of Wilson lines and deconfinement*, Phys. Rev. D 74 (2006) 121703 [hep-ph/0608242].
- [20] A. Vuorinen and L.G. Yaffe, *$Z(3)$ -symmetric effective theory for $SU(3)$ Yang-Mills theory at high temperature*, Phys. Rev. D 74 (2006) 025011 [hep-ph/0604100]; A. Kurkela, *Framework for non-perturbative analysis of a $Z(3)$ -symmetric effective theory of finite temperature QCD*, Phys. Rev. D 76 (2007) 094507 [arXiv:0704.1416]; Ph. de Forcrand, A. Kurkela and A. Vuorinen, *Center-symmetric effective theory for high-temperature $SU(2)$ Yang-Mills theory*, Phys. Rev. D 77 (2008) 125014 [arXiv:0801.1566].
- [21] K. Farakos, K. Kajantie, K. Rummukainen and M. Shaposhnikov, *3d physics and the electroweak phase transition: a framework for lattice Monte Carlo analysis*, Nucl. Phys. B 442 (1995) 317 [hep-lat/9412091].
- [22] M. Laine and A. Rajantie, *Lattice-continuum relations for 3d $SU(N)$ +Higgs theories*, Nucl. Phys. B 513 (1998) 471 [hep-lat/9705003].
- [23] K. Kajantie, M. Laine, K. Rummukainen and Y. Schröder, *Four-loop vacuum energy density of the $SU(N_c)$ + adjoint Higgs theory*, JHEP 04 (2003) 036 [hep-ph/0304048].
- [24] G.D. Moore, *$O(a)$ errors in 3-D $SU(N)$ Higgs theories*, Nucl. Phys. B 523 (1998) 569 [hep-lat/9709053].

- [25] K. Kajantie, M. Laine, K. Rummukainen and Y. Schröder, *How to resum long-distance contributions to the QCD pressure?*, Phys. Rev. Lett. 86 (2001) 10 [hep-ph/0007109].
- [26] G.N. Watson, *Three triple integrals*, Q. J. Math. 10 (1939) 266; M.L. Glasser and J. Boersma, *Exact values for the cubic lattice Green functions*, J. Phys. A: Math. Gen. 33 (2000) 5017.
- [27] F. Di Renzo, E. Onofri, G. Marchesini and P. Marenzoni, *Four loop result in SU(3) lattice gauge theory by a stochastic method: lattice correction to the condensate*, Nucl. Phys. B 426 (1994) 675 [hep-lat/9405019].
- [28] F. Di Renzo and L. Scorzato, *Numerical Stochastic Perturbation Theory for full QCD*, JHEP 10 (2004) 073 [hep-lat/0410010].
- [29] H. Panagopoulos, A. Skouroupathis and A. Tsapalis, *Free energy and plaquette expectation value for gluons on the lattice, in three dimensions*, Phys. Rev. D 73 (2006) 054511 [hep-lat/0601009].
- [30] G. Parisi and Y.S. Wu, *Perturbation theory without gauge fixing*, Sci. Sin. 24 (1981) 483.
- [31] J.C. Sexton and D.H. Weingarten, *Hamiltonian evolution for the hybrid Monte Carlo algorithm*, Nucl. Phys. B 380 (1992) 665.
- [32] P. Arnold and O. Espinosa, *The effective potential and first order phase transitions: Beyond leading-order*, Phys. Rev. D 47 (1993) 3546; *ibid.* D 50 (1994) 6662 (Erratum) [hep-ph/9212235]; E. Braaten and A. Nieto, *Effective field theory approach to high temperature thermodynamics*, Phys. Rev. D 51 (1995) 6990 [hep-ph/9501375].
- [33] M. Lüscher and P. Weisz, *Coordinate space methods for the evaluation of Feynman diagrams in lattice field theories*, Nucl. Phys. B 445 (1995) 429 [hep-lat/9502017].
- [34] S. Necco and R. Sommer, *The $N_f = 0$ heavy quark potential from short to intermediate distances*, Nucl. Phys. B 622 (2002) 328 [hep-lat/0108008].
- [35] K. Farakos, K. Kajantie, K. Rummukainen and M.E. Shaposhnikov, *3D physics and the electroweak phase transition: Perturbation theory*, Nucl. Phys. B 425 (1994) 67 [hep-ph/9404201].
- [36] A.K. Rajantie, *Feynman diagrams to three loops in three-dimensional field theory*, Nucl. Phys. B 480 (1996) 729; *ibid.* B 513 (1998) 761 (Erratum) [hep-ph/9606216].
- [37] S. Groote, J.G. Körner and A.A. Pivovarov, *Laurent series expansion of sunrise-type diagrams using configuration space techniques*, Eur. Phys. J. C 36 (2004) 471 [hep-ph/0403122].

exact					
am_3	d_{00}	d_{10}	d_{11}	d_{21}	d_{22}
0.25	0.92893	2.9249	0.13737	2.7649	-0.19780
0.30	0.91214	2.7230	0.13855	2.6428	-0.17972
0.40	0.87839	2.3909	0.13998	2.4058	-0.15127
0.50	0.84462	2.1210	0.14017	2.1949	-0.12936
0.60	0.81103	1.8924	0.13919	2.0074	-0.11150
0.80	0.74518	1.5201	0.13422	1.6830	-0.083553
1.00	0.68209	1.2285	0.12612	1.4072	-0.062617
1.00*	0.68209	1.2285	0.12612	1.8283	-0.086011

fitted					
am_3	d_{00}	d_{10}	d_{11}	d_{21}	d_{22}
0.25	0.9299(6)	2.923(3)	0.1362(6)	2.74(4)	-0.199(2)
0.30	0.9110(7)	2.720(3)	0.1384(5)	2.63(3)	-0.177(2)
0.40	0.8782(4)	2.392(2)	0.1392(3)	2.39(1)	-0.1509(7)
0.50	0.8451(3)	2.122(1)	0.1403(4)	2.191(6)	-0.1292(4)
0.60	0.8113(5)	1.893(1)	0.1384(4)	1.994(6)	-0.1110(4)
0.80	0.7455(1)	1.5223(2)	0.13414(7)	1.683(1)	-0.08345(7)
1.00	0.6823(1)	1.2309(2)	0.12614(5)	1.4077(7)	-0.06255(5)
1.00*	0.6822(3)	1.230(1)	0.1261(1)	1.829(3)	-0.08596(16)

fitted					
am_3	d_{20}	d_{30}	d_{31}	d_{32}	d_{33}
0.25	16.49(3)	109.4(4)	7.2(7)	-2.16(6)	-0.060(19)
0.30	14.09(3)	81.8(3)	9.6(3)	-1.73(5)	-0.038(10)
0.40	10.87(1)	52.2(1)	9.4(1)	-1.27(1)	-0.029(3)
0.50	8.74(1)	36.7(1)	8.61(5)	-0.916(7)	-0.0201(7)
0.60	7.18(1)	27.2(1)	7.59(5)	-0.670(6)	-0.0155(5)
0.80	5.058(2)	16.11(2)	6.035(7)	-0.3522(9)	-0.01423(6)
1.00	3.664(1)	10.16(1)	4.652(4)	-0.1605(5)	-0.01327(3)
1.00*	3.666(6)	10.19(6)	6.46(2)	-0.196(3)	-0.01677(11)

Table 2: The coefficients d_{ij} (cf. Eq. (4.3)) in the infinite-volume limit. The starred mass refers to $\ln \beta = \ln 80$; the others to $\ln \beta = \ln 24$. The numbers in parentheses indicate the statistical errors of the last digits shown.

coefficients	$a_{ij}^{(0)}$	$a_{ij}^{(1)}$	$a_{ij}^{(2)}$	$a_{ij}^{(3)}$	$\chi^2/\text{d.o.f.}$
* ϕ_{00}^r	-0.039789	-0.0062086	0.0056620	-0.00076693	—
* ϕ_{10}^r	0.038310	-0.014881	-0.00082279	0.0029967	—
* ϕ_{11}	0.015831	0.0076464	-0.0094444	0.0017264	—
ϕ_{20}	0.0092578	0.027798	-0.039072	0.014739	55.07
* ϕ_{21}	0.010909	0.014947	-0.0022681	-0.0043976	—
* ϕ_{22}	-0.0053827	-0.0050144	0.0074469	-0.0014995	—
ϕ_{30}	0.0024038	0.0071490	-0.0020206	-0.0016577	19.83
ϕ_{31}	0.0013885	-0.0035354	0.024195	-0.013013	0.996
ϕ_{32}	-0.0018767	-0.0049224	0.0013548	0.0029473	1.966
ϕ_{33}	-0.00031675	-0.00036476	-0.00032547	-0.00014179	1.063
* $\tilde{\phi}_{21}$	0.0075590	0.0023970	-0.0033645	0.00069377	—
* $\tilde{\phi}_{22}$	-0.0025197	-0.00079883	0.0011212	-0.00023111	—
* $\tilde{\phi}_{31}$	0.0036091	0.0031005	-0.00069559	-0.00088573	—
* $\tilde{\phi}_{32}$	-0.0012030	-0.0026312	0.0043532	-0.0011224	—
* $\tilde{\phi}_{33}$	0.0	0.00053248	-0.0013736	0.00047246	—

Table 3: The fit coefficients allowing to estimate the functions ϕ_{ij} , $\tilde{\phi}_{ij}$ in the range $0.0 \leq am_3 \leq 1.0$, according to Eq. (5.7). In the cases marked with a star, the fits have been carried out to the exact results rather than to NSPT data (we cite no $\chi^2/\text{d.o.f.}$ here because no error bars can be assigned to the exact numbers); the accuracy of their description through a polynomial fit is on the per cent level.

coefficients	$b_{ij}^{(0)}$	$b_{ij}^{(1')}$	$b_{ij}^{(1)}$	$b_{ij}^{(2)}$	$b_{ij}^{(3)}$	$\chi^2/\text{d.o.f.}$
ϕ_{20}	0.0092578	0.0097310	0.0090404	-0.010317	0.0047392	0.128
ϕ_{30}	0.0024038	-0.0036880	0.014462	-0.013444	0.0024569	1.185
ϕ_{31}	0.0013885	-0.0017147	-0.00022591	0.019122	-0.011248	0.932
ϕ_{32}	-0.0018767	0.0058403	-0.016324	0.018943	-0.0032415	0.361
ϕ_{33}	-0.00031675	-0.0029965	0.0052048	-0.0086842	0.0026476	0.737

Table 4: The fit coefficients allowing to estimate the functions ϕ_{20} , ϕ_{30} , ϕ_{31} , ϕ_{32} , ϕ_{33} in the range $0.0 \leq am_3 \leq 1.0$, according to Eq. (5.8).